621.385.833

ELECTRON MICROSCOPY OF THE MAGNETIC STRUCTURE OF THIN FILMS

V. I. PETROV, G. V. SPIVAK, and O. P. PAVLYUCHENKO

Moscow State University; Physics Institute, Siberian Division,
USSR Academy of Sciences, Krasnoyarsk

Usp. Fiz. Nauk 106, 229–278 (February, 1972)

The review is devoted to a description of the possibilities afforded by transmission electron microscopy for the investigation of magnetic structures of thin ferromagnetic films, and presents experimental data on magnetic films obtained by using a transmission electron microscope. We consider and compare different microscope operating regimes for observing the magnetic structure. The formation of the contrast of the magnetic structures in the most widely used modes, namely the defocusing mode and the small-angle electron diffraction mode, are considered in detail. Particular attention is paid to obtaining data on the domain walls and the fine structure of the magnetization inside the domains. Different methods of measuring the widths of the boundaries are compared, and the possible sources of errors are discussed. The prospects for using ultra-high voltage electron microscopes for the investigation of thicker films are noted. Experimental data are given on the investigation of domain configurations in single-crystal foils and in polycrystalline films, and the dependences of the magnetic parameters of the film on the structure and on the conditions of obtaining the films are discussed. Results of an investigation of a quasistatic and pulsed remagnetization of magnetic films are described.

CONTENTS

THE interest in thin magnetic films is due to the possibility of their extensive practical utilization and to a number of features that distinguish them from bulky ferromagnets. Among the different means of investigating their magnetic structure[1-5], the transmission electron microscope occupies an important place[2-9]. This is due to the high resolution of the instrument, to the good contrast, and to the relative ease of interpreting the image. An electron microscope yields local quantitative data on the magnetic structure and the parameters of the film in static and dynamic regimes.

The use of electron-optical methods for the investigation of magnetic structures on the surfaces of bulky samples is considered in the review[10].

I. OPERATING MODE OF TRANSMISSION MICROSCOPE WHEN PRODUCING PICTURES OF THE MAGNETIC STRUCTURE OF THIN MAGNETIC FILMS

A feature of the observation of the magnetic structure of TMF is that when the instrument is focused on the sample and when the aperture diaphragm is centered, there is no image of the magnetic structure (the electron deflection due to the magnetization inside the film is $\sim 10^{-4}$ rad, and the deflected electrons are not stopped by the aperture diaphragm). As shown in[11,12], the magnetic structure is seen by the electron waves as a pure phase object. The phase shift between two rays that start out from the same point and converge at another point, but travel along different paths, is equal to $2\pi e\Delta\Phi/ch$, where e is the electron charge, c is the velocity of light, h is Planck's constant, and $\Delta\Phi$ is the total magnetic flux between these two paths. The fact that the phase shift is determined not by the Lorentz force but by the flux was demonstrated experimentally[13-20] by observation of electronic interference patterns. To observe pure phase objects in electron microscopy, just as in ordinary microscopy, it is necessary to have special operating conditions. This explains why the transmission microscope came into use for the observation of thin-magnetic-film structures only relatively recently[21-24]. At the present time, practically all the commercial microscopes are adapted for such observations[21,24-39].

1. Defocusing method. In this regime, a plane located at a distance Z above (underfocusing) or below (overfocusing) the film plane is projected on the screen. The interaction with the magnetization M_S in the film leads to a redistribution of the electron trajectories and to appearance of contrast on the screen (Fig. 1). The domain walls appear on the image in the form of dark and bright lines (see, e.g., Fig. 12 below), depending on the direction of the magnetization on both sides of the wall. The walls represented by dark lines are

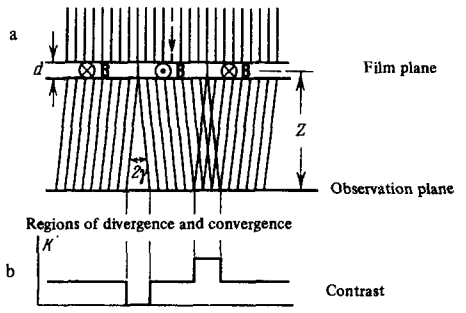

FIG. 1. Defocused operating mode of transmission electron microscope. a) Electron trajectory on passing through a magnetic film containing several 180° domain walls; b) contrast in the observation plane.

called "diverging" and those by light lines "converging." The change of the direction of the magnetization inside the domain (the fine structure of the magnetization of the domain or the ripple of the magnetization) appears on the image in the form of thin light and dark wave-like lines perpendicular to M_S[40]. This is used for an exact determination of the local direction of M_S. This method was used in[41] to obtain the distribution of M_S in film spots of 1–50 μ diameter. In[380] it was proposed to use as a memory element a film having circular anisotropy inside each square of a grid as a result of which these squares of the films acted as a converging or a diverging lens. The direction of M_S at the edges of the film can be determined also from the border produced on the image[42-44]. On going from the overfocusing to the underfocusing mode and back, and also when the film is rotated, the contrast of the image is reversed. The latter was chosen to separate magnetic and structural diffraction effects[45]. The magnitude of the defocusing is chosen in accordance with the object and scope of the research and can fluctuate from fractions of a millimeter to several dozen centimeters.

Defocusing causes a certain lowering of the resolution of the microscope, but usually the resolution is limited by the aperture of the illuminating source. By using condensers with large optical strength[46] or by using small condenser diaphragms (down to 5 μ)[26-28], a resolution of ~1000 Å and higher is reached[36,46-50]. At small illuminator apertures, the image brightness is small and long exposures are required. A considerable gain in image brightness and quality is obtained with a point cathode, in which the emission density is 10^3–10^4 times larger than from a thermionic cathode[51,28,46,52]. The use of a point cathode and overfocusing of a two-lens condenser[53] have made it possible to obtain a source aperture of 5×10^{-7} rad.

When working with a small-aperture source, the requirements on the operating stability of all the microscope units become much more stringent. The power supply is therefore made more stable, one operates at a reduced accelerating voltage, and the vibrations of the column are minimized[54].

To eliminate the influence of the stray field of the magnetic lenses, the sample is usually raised 20–30 mm above its usual position[55,56], or else a specially shaped pole piece is used[47,57]. It is also possible to operate with the objective lens turned off, but in this case the resolution is low and the magnification is small[58,59]. On the other hand, when the object is placed above the objective lens, a larger magnification and better resolution are obtained, but the magnitude of the defocusing is small, and consequently the sensitivity to small changes of the magnetic structure of the film is low. Large defocusing with good resolution can be obtained by placing the object between the objective and the intermediate lenses[60]. The objective can then be used as an additional condenser lens and the aperture of the illumination can be decreased by approximately a factor of 20.

In spite of the fact that the contrast is not produced by the aperture diaphragm, the presence of the diaphragm does greatly influence the contrast. The diaphragm cuts off the background of the stray electrons, thereby increasing the magnetic contrast. Its use is particularly important in the investigation of thick films[61]. The axial position of the diaphragm must be determined by trial, since it can limit the field of view when working with different excitations of the objective[46,40].

The maximum sample thickness at an accelerator voltage 100 kV is 1000–2000 Å[26,61]. The structure of a thick object cannot be recorded by increasing the photographic exposure, since the increased inelastic scattering of the electrons makes the resolution worse and lowers the contrast. Microscopes with higher accelerating voltages make it possible to investigate thicker films[38,62].

2. Ray-intercept method. In this case the microscope operates in the in-focus mode and contrast of domains with different magnetizations is produced with the aid of a special knife-edge diaphragm (or a displaced aperture diaphragm) located in the rare focal plane of the objective[63].

Owing to the interaction of the electrons with the magnetization, the diffraction picture is split. The diaphragm holds back the electrons passing through domains with definite magnetization directions (Fig. 2), and these domains appear dark in the picture. The image reveals simultaneously the magnetic structure and the geometry of the film. The pictures are similar to those obtained by the magneto-optical method, but the contrast and sharpness are higher.

For good contrast, the knife edge should be parallel to the magnetization vectors in the film, and the aperture diaphragm should be shifted perpendicularly to the 180° walls. The displacement of the diaphragm changes the contrast sharply, and since the distance between the

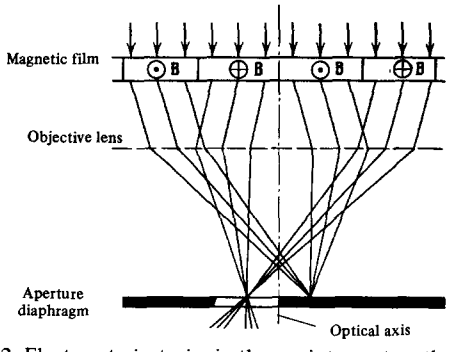

FIG. 2. Electron trajectories in the ray-intercept method.

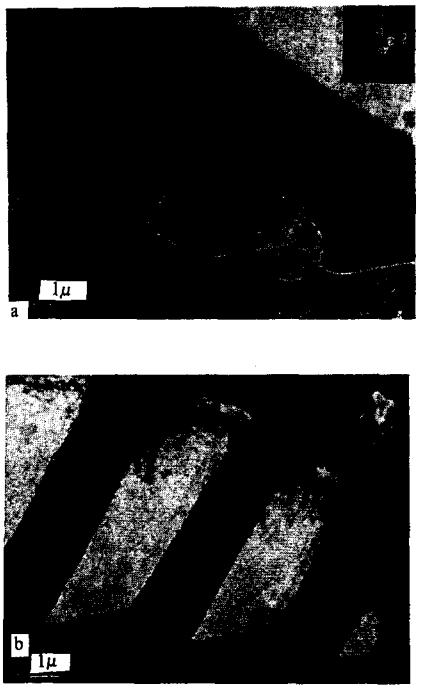

FIG. 3. Electron micrographs of a foil of Fe + 4% Si. a) Defocused image, the domains 1, 2, and 3 correspond to spots on the electron diffraction pattern from the circular region of the sample marked on the photograph; b) picture obtained by the ray-intercept method (the position of the diaphragm is shown dashed on the picture); the domains corresponding to spot 1 are dark in the picture [65].

crossovers is very small (~1 μ), the position of the edge must be set with high accuracy. Different methods of microscope operations in this regime are considered in[64].

Very good images (Fig. 3) were obtained by using as the knife edge a thin tungsten filament (7 μ diameter) fastened on the aperture diaphragm (the aperture diaphragm itself did not participate in the interception of the rays, and was mounted on the optical axis). The small dimensions of the knife and the possibility of displacing the diaphragm along the axis of the system ensured good selectivity. By blocking different diffraction reflections with the filament, it is possible to obtain light-field and dark-field images of the domains[65,66]. The developed magnetization-reversal device has made it possible to observe magnetization reversal at large magnifications[67].

The ray-intercept method is difficult to use for the study of an irregular domain structure, with small-angle and wavy walls, when it is necessary to choose a suitable position of the knife-edge diaphragm. A modification of the intercept method is proposed in[369].

3. Method of quarter-wave plate and interference microscopy. The possibility of using other methods of phase microscopy for observing magnetic structures, namely the method of quarter-wave plate and the method of interference microscopy, pointed out in[68,69]. The realization of these methods entails considerable difficulties. It is possible that some of them can be overcome by using holography[70] and performing some of the operations outside the microscope[68]. Theoretical calculations on the use of holography in Lorentz microscopy are given in[71].

An interesting method was proposed in[72]. A phase-shifting carbon film ~100 Å thick is placed in the focal plane of the objective lens. The contrast is produced by the different scattering of the electrons in the film.

4. Small-angle electron diffraction. A modification of the defocusing method is the method of small-angle electron diffraction. In this case the defocusing is very large. The method of small-angle diffraction was used earlier to investigate organic molecules and the structures of thin films[73], and it was shown that this regime yields more information than an ordinary electron-microscope. The region observed in the small-angle diffraction mode is concentrated near the central spot. In this mode the camera must be very long and the angular resolution high. This can be ensured by different methods. The review[74] gives different schemes of microscope operation in this regime. At an accelerating voltage of 100 kV, a camera length up to 150 m was obtained[75]. The resolution in the small-angle diffraction mode turned out to be 2×10^{-6} rad using an ordinary cathode[75] and 5×10^{-7} rad using a point cathode[53].

Regions of magnetic films with large dispersion of the magnetization direction were observed in the small-angle electron diffraction mode with small angular resolution[76,77]. At a better angular resolution, diffraction was observed by a periodic magnetic structure with a period ~1 μ, which is the regular structure of antiparallel domains in Co foils with anisotropy axis making an angle with the foil plane (Fig. 4) and in cross-tie walls in permalloy films[75,78,79].

5. Method of extinction and bend contours. In investigations of single-crystal foils in a transmission microscope, the image always reveals extinction contours, each of which is connected with Bragg reflection from a definite plane. In the investigation of magnetic materials, the Lorentz force, which deflects the electrons and alters their incidence angle on the crystallographic planes, alters by the same token the conditions of the Bragg reflection. Since the deflection by the magnetic field is small compared with the Bragg angles

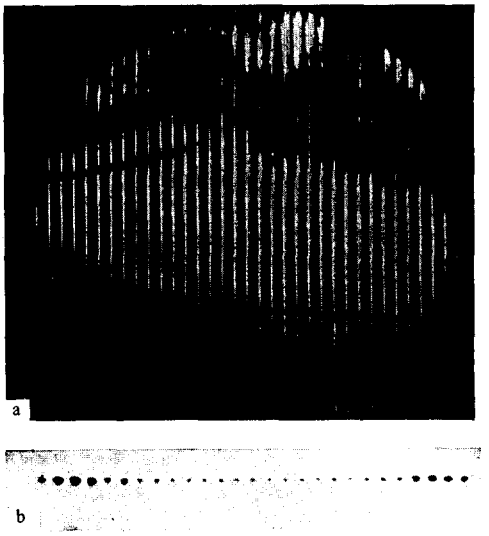

FIG. 4. a) Defocused image of Co foil, showing a regular structure of antiparallel domains; b) image of this structure in the small-angle electron diffraction regime [78].

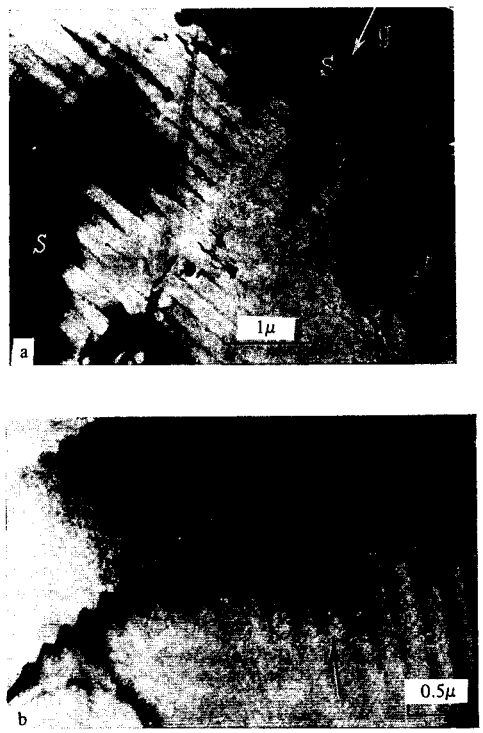

FIG. 5. Distortion of extinction contours on domain structures. a) Single-crystal Co, appearance of "steps" on the contour [80]; b) Fe (111) foil with strip domains, appearance of "zig-zags" on the contour (A. Bourret and M. Kleman, unpublished photograph [69]).

(~0.01), this leads only to a distortion of the contour, something observed on Co and Ni foils[80,81]. Two types of effects were observed, a stepwise change of the position of the contour from domain to domain, and the appearance of zig-zags on the contour (Fig. 5). The steps on the contour are due to the changes, in the domains, of the M_S component parallel to the plane of the sample. The jumps of the contour occur on the domain walls. The zig-zags on the contour appear only in the presence of a magnetization-vector component perpendicular to the film. This effect is determined by the magnetic flux both inside and outside the film. In this case the domain boundary corresponds to the maximum displacement of the contour. Since the normal component of the magnetization vector is connected with magnetic charges on the surface of the film, this effect makes it possible to display the locations of the charges on the surface of the film with quite high sensitivity.

The diffraction contrast from a ferromagnetic crystal is calculated in[81-83].

II. IMAGE CONTRAST OF MAGNETIC STRUCTURES

We consider the formation of the contrast only in the most frequently employed operating microscope modes, namely the defocusing mode and the small-angle diffraction mode (see also[370]). The action of factors that lead to distortion of the contrast and limits the resolution will be considered in the next chapter.

A rigorous solution of the problem of the contrast from a magnetic structure is obtained with the aid of wave optics. The intensity of the image of the magnetic structure of the film, which is a phase object for the electron wave, is obtained by the usual methods of diffraction theory[18-20,84]. The theory of the contrast of the magnetic structure of films was further developed in[85-87,68]. The contrast of the flux lines in type-II superconductors[87,88], which were experimentally observed in[89], was also calculated.

Let us derive an expression for the contrast, for a film of thickness d with one-dimensional distribution of the magnetization $\mathbf{M}_S(\xi)$, illuminated by a point source of electrons (Fig. 6). For a ray passing through a certain point ξ on the 0ξ axis, the phase-shifting action of the magnetic structure of the film is determined by the magnetic flux through the section of the film between the origin and the point ξ (Fig. 6, shaded surface):

$$\Delta\varphi = -\frac{ed}{\hbar}\int_0^{\xi} B_\eta(\xi)\,d\xi. \tag{1}$$

The excitation at the point x on the observation plane is recorded in the form of a Kirchoff integral.

In the Fresnel approximation, corresponding to the defocusing regime, we have

$$u(x) = A\exp\left[ik\left(Z+S+\frac{x^2}{2Z}\right)\right]\int_{-\infty}^{+\infty} R(\xi)\exp[i\Omega(\xi)]\,d\xi, \tag{2}$$

where

$$\Omega(\xi) = -\frac{kx\xi}{Z}+\frac{k(Z+S)}{2ZS}\xi^2, \quad R(\xi)=\exp[i\Delta\varphi(\xi)], \quad k=2\pi/\lambda,$$

$\lambda = h/mv$ is the electron wavelength, v and m are the velocity and mass of the electron, and A is a constant. The contrast in the observation plane is defined as $K(x) = |u(x)|^2/|u_0|^2$, where $|u_0|^2$ is the intensity in the absence of a magnetic structure.

Expression (2) leads, as a first approximation, to the formulas obtained for the contrast from geometrical optics[40,49]:

$$K(x) = \left(1+\frac{ZS}{Z+S}\frac{d\gamma_\xi}{d\xi}\right)^{-1}, \tag{3a}$$

$$x = \frac{Z+S}{S}\xi + Z\gamma_0\frac{M_\eta}{M_S} = \frac{Z+S}{S}\xi + Z\gamma_\xi, \tag{3b}$$

where $\gamma_0 = 4\pi dM_S(e/2mU)^{1/2}/c$ is the total angle of deflection of the electron when it interacts with M_S, and U is the accelerating voltage.

Expressions (3) are much simpler and more convenient than (2), but they are not always correct. The limit of applicability of geometrical optics yields the expression obtained in[90] as the condition for the validity of the stationary-phase method:

$$\frac{ed}{hc}|B''(\xi)| < \frac{3}{\sqrt{n}}\left|\frac{1}{\lambda Z}+\frac{ed}{hc}B'(\xi)\right|^{3/2}, \tag{4}$$

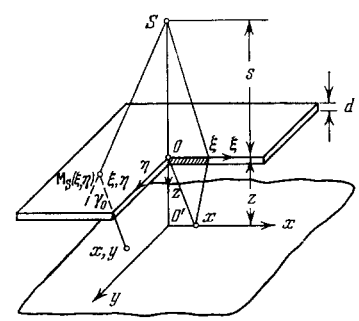

FIG. 6. For use in the calculation of the contrast in the defocused regime.

where n is the number of Fresnel zones. The limit of applicability of geometrical optics, obtained in[85] from the uncertainty relation, is $\Delta\Phi \geq h/2e$ ($\Phi_0 = h/2e = 2.07 \times 10^{-7}$ G/cm^2 is the minimum change of the magnetic flux that can still be determined with the aid of geometrical optics) and is rigorously valid only in the case of Fraunhofer diffraction.

The Fraunhofer approximation of the Kirchhoff integral corresponds to the regime of small-angle electron diffraction:

$$u(x) = A \int_{-\infty}^{+\infty} R(\xi) \exp\left(-i k \frac{\xi x}{Z}\right) d\xi. \qquad (5)$$

If the film contains a regular domain structure, then its action on the electron flux is equivalent to the action of diffraction gratings in optics. Figure 7 shows a film with antiparallel periodic domains, its phase characteristic, and diffraction picture. The position of the diffraction peaks is determined by the period of the lattice (a/2). The envelope of the intensity of the peaks has a maximum at $s_1 = \pm\Delta_0/2a$, which corresponds to the Lorentz deflection ($\gamma_0 = \lambda s_1 = \lambda d e B_\eta / ch$). This agrees with the experimental data. If the resolution is insufficient, then there are no diffraction maxima between the maxima determined by the Lorentz deflection, and we see in their place a straight strip of decreased intensity. It was also noted that the contrast of the image of the periodic domain structure is reversed[75] when the defocusing is continuously varied.

When the Lorentz deflection angle and the domain widths are small (e.g., for $CrBr_3$[91], where $2a \approx 1000$ Å and $B_\eta = 1500$ G), the peaks corresponding to the Lorentz deflection are not seen on the diffraction picture. It contains only maxima due to the lattice—a large zero-order maximum and two side lobes; in addition, the diffraction picture is not symmetrical. The asymmetry of the picture may be due to the unequal widths of the domains with opposite magnetization directions, which leads to asymmetry of the structure factor B(s) and causes asymmetry in the distribution of the intensity[92]. The experimental intensities do not coincide with the calculated ones and are much larger than the latter. This disparity is not eliminated by using different distributions of the magnetization in the domains and different widths of the domain walls. This effect can be due to an error in the determination of the inclination of the foil, as a result of its bending, and to small-angle inelastic scattering of the electrons, which was not taken into account[91].

Theoretical calculations of the image in the Fraunhofer diffraction were also carried out for other objects, antiferromagnets and type-II superconductors with regular flux-line structure[79].

By operating in different regimes, it is possible to observe also very small magnetic inhomogeneities ($\Delta\Phi \ll \Phi_0$), but, as shown in[93], the number of electrons necessary to register the image is different. The point is that at $\Delta\Phi \gg \Phi_0$ almost all the electrons are scattered by the same inhomogeneity, whereas when $\Delta\Phi \ll \Phi_0$ practically none of the electrons interact with the field. And since the accuracy of the registration is determined by the number of detected electrons, it follows that to register magnetic inhomogeneities with high accuracy at $\Delta\Phi \ll \Phi_0$ it is necessary to have a large number of electrons, i.e., longer exposure times. The exposure time calculated for such inhomogeneities with the aid of wave optics is appreciably larger than that obtained from classical concepts[94].

III. STUDY OF DOMAIN-WALL STRUCTURE

1. **Types of boundaries in thin magnetic films.** At the present time there is a considerable number of theoretical calculations of the structure of domain walls[95-107], where different models of the domain wall are considered or proposed. In some papers, a one-dimensional model is used and analytic expressions are obtained connecting the parameters of the wall and of the film, while in others the walls considered are more complicated and the calculation is performed with an electronic computer. In particular, two-dimensional models with inhomogeneous distribution of the magnetization over the thickness were investigated[106,107]. A model in which there are no stray fields is considered in[107]. There is a review[371] devoted to calculations of the structure of the walls. Plots of the domain-wall width against the film thickness for several models are shown in Fig. 8. In comparing data by different authors, both theoretical and experimental, it is necessary, however, to take into account the fact that the domain wall may be differently defined in different papers.

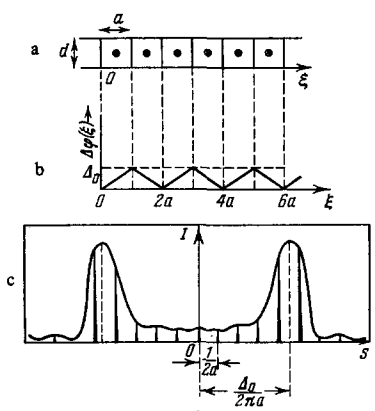

FIG. 7. Small-angle electron diffraction. a) Cross section of film with periodic structure of antiparallel domains; b) change of phase for structure (a); c) distribution of intensity of the image of the phase grating (a) in the small-angle diffraction mode [75].

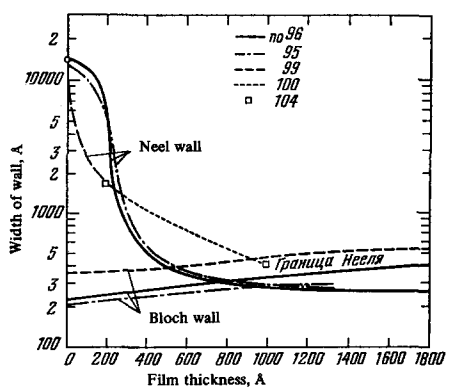

FIG. 8. Theoretical plots of the domain-wall width against the film thickness, obtained by different authors for 80% Ni-Fe, $M_S = 800$ G, $A = 10^{-6}$ erg/cm, $K = 10^3$ erg/cm [147].

In very thin films, the Neel walls are energywise favored, and in thick films the Bloch walls are favored (in the former case M_S, while rotating in the wall, remains in the plane of the film, and in the latter it goes out of the plane of the film and remains in the plane of the wall). In films of intermediate thickness, a transition type of wall is favored, namely a wall with cross ties or of the "barbed wire" type, consisting of segments of Bloch walls and Neel walls. Its model, obtained from powder patterns[108], was later confirmed by investigations in an electron microscope[36]. The distance between the cross ties is 1–10 μ, and their density increases with increasing anisotropy field H_k and depends on the thickness of the film (it is maximal at d ≈ 600 Å[26]). In later investigations[109], no correlation was obtained between the cross-tie density and the film thickness. Demagnetization with an alternating field gave a density scatter up to a factor of 6. When the wall approaches defects, the density changes by a factor 3–4.

Mutual conversions of homogeneous walls into walls with cross ties were observed by heating a film[110,111] and by changing the "number of degrees" of the walls by stretching[112-114] (homogeneous Neel walls with $2\alpha < 180°$ changed into 180° walls with cross ties upon stretching), and under the action of a field along the difficult-magnetization axis[115], where the transition was due to a displacement of the Bloch lines and was obtained at different angles α with increasing and decreasing field. Under the action of the field along the difficult magnetization axis, the configuration of the wall with cross ties changed, and hysteresis of the displacement of the Bloch lines was observed[116]. When the angle of the walls changed, the width of the wall decreased with decreasing 2α only for thin films (d < 120 Å). For thicker films, the width of the walls

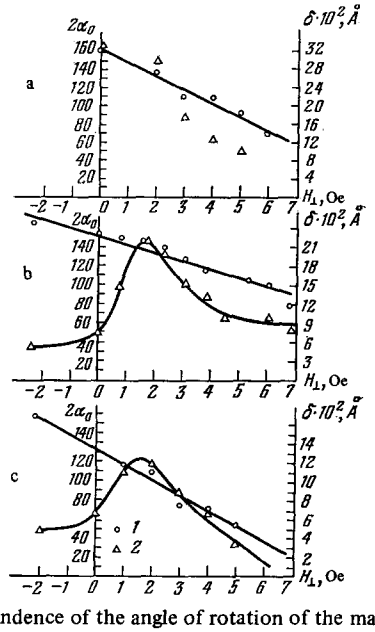

FIG. 9. Dependence of the angle of rotation of the magnetization in the wall (2α) and the width of the wall (δ) on the magnetic field along the difficult magnetization axis ($H_\perp$). a) d = 120 Å, H_k = 8.3 Oe, H_c = 5 Oe; b) d = 250 Å, H_k = 7.3 Oe, H_c = 4.2 Oe; c) d = 530 Å, H_k = 6.2 Oe, H_c = 2.5 Oe [117].

was maximal at 2α = 120–140° (Fig. 9). The presence of such a relation is apparently connected with the change in the wall structure[117]. This is also indicated by investigations in the small-angle electron diffraction mode[118].

A theoretical analysis predicts the existence of walls of a definite type only in a definite range of film thicknesses. There are grounds, however, for assuming that this is not the case[119,101,103]. In particular, there is a critical value of the angle between the magnetizations in the neighboring domains ($2\alpha_{cr}$), when walls with $\alpha > \alpha_{cr}$ are not revealed by powder for thick films (d ≈ 1200 Å), whereas for $\alpha < \alpha_{cr}$ the walls can be clearly seen with the aid of powder. This can be easily explained by changing over from Bloch walls, which attract the powder weakly, to Neel walls, which have large stray fields[120]. A theoretical analysis of the transitions between the Bloch and Neel walls[119,101,103] has shown the following: 1) below a definite thickness, only Neel walls exist in the films, 2) at large thicknesses, the Neel walls appear at $\alpha < \alpha_{cr}$, at $\alpha_{cr} < \alpha < \pi/2$ there are only intermediate walls, and only at $\alpha = \pi/2$ do pure Bloch walls exist. Pure Bloch walls ($\alpha = \pi/2$) were observed in thick (1200–2000 Å) homogeneous fine-grain permalloy films. After annealing the films, the angle of rotation of the magnetization in the wall was no longer equal to 180°, owing to the growth of the crystallites, and the angle varied along the wall. This caused the appearance of an alternating Neel component along the wall and formation of cross ties[61,121]. In[122] there was observed the formation of cross ties on a Neel wall passing inside individual crystallites of a large-grain Ni-Fe film.

Most experiments aimed at the investigation of the walls did not result in limitations with respect to the film thickness for the existence of domain walls of any particular type. Boundaries with cross ties were observed both in very thin films (d = 30–180 Å)[123] and in thick ones[101,102], although in some cases[97,124] they were observed only at d < 1000 Å. The effect of polarity in a field perpendicular to the film, which was observed for films of thickness 200–1600 Å, and the dependence of the domain-wall width on this field, point to the presence of the Bloch component in the walls[125]. For Ni films of thickness 200–800 Å with perpendicular anisotropy at $K_\perp > K_{\perp cr}$, the walls were of the Bloch type, which coincides with the energy calculations; for $K_\perp < K_{\perp cr}$, the walls became of the Neel type[126,127].

Walls with cross ties were observed in polycrystalline films. Thus, in Fe films, where both 90° and 180° walls existed, the cross ties appeared on the 180° walls at d < 1000 Å, and at d < 400 Å walls with cross ties predominated. On 90° walls, no cross ties were observed[128,129]. In epitaxial electrically-deposited films of Ni-Fe with domain structure of the checkerboard type, cross ties were also observed on the boundaries[130].

In single-crystal films of Fe, Ni, and β-Co, the type of wall was determined by heating[131]. The ratio of the contributions of the different energies was varied thereby, and if the wall was of the Neel type, it did not change, but if it was of the Bloch type, then it acquired Neel sections. It was observed that the 180° walls are of the Bloch type in Fe and β-Co films at d > 80 Å. In

Ni films (d = 300–500 Å), the 180° walls had both Bloch and Neel sections.

Interesting data were obtained in the investigation of thick epitaxial films of Fe (0.1–1.0 μ) in a super-high-voltage electron microscope with accelerating voltage 1000 kV[62,132]: a) at d > 1000 Å the Neel boundaries go over into Bloch walls; b) at d = 1000–3000 Å, asymmetrical 180° walls are observed, and their contrast coincides quite well with the contrast calculated for the model of[107]; c) considerable changes in the width of the image of the 90° wall were observed, this being attributed to different inclinations of the different sections of the wall relative to the film plane.

In addition to the walls with $2\alpha \leq 180°$, there were observed also 360° walls, which occur in thin films with d < 300 Å (the 360° walls are energywise more convenient for thin films[133]), and the origin of which is connected with the prior history of the sample. The formation of such walls during the course of magnetization reversal was observed[134] in films of 80% Ni-Fe evaporated without a field, and also on sections of a film with radial anisotropy, which was produced after the film was annealed by an electron beam focused on the sample[48,135]. A detailed electron-microscope investigation of the 360° walls was carried out in[136]. The formation of such walls was attributed to the fact that the mobility of the Bloch lines is smaller than in thick films. Owing to the absence of stray fields, the 360° walls can be strongly bent, even closed, and experience changes only under the influence of rather strong fields (~100 Oe), when the motion of the Bloch lines becomes possible. An analysis of the walls by the procedure of[49] has shown that the true 360° boundary (the magnetization vector rotates continuously through 360°) takes place when the magnetization in neighboring domains is perpendicular to the wall. If the angle differs from 90°, then at two places of the wall the magnetization vector is perpendicular to the wall, and it can be regarded as two 180° walls that come closer together. Such double walls can occur when the wall curls around an inclusion[137].

The formation of unusual domain walls with neighboring-domain magnetizations directed perpendicular to the wall was observed in films of permalloy[138], Fe, and Co[139], after applying a rather strong magnetic field perpendicular to the film. The formation of such a structure is attributed to the presence of a geometric relief in the film. The width of such walls is quite large (5–8 μ), and inside the wall there is observed a fine magnetic structure, a magnetization ripple with wavelength larger than in the remaining parts of the film[139]. Calculation performed for a simple model of the walls[138] explained the contrast of the image of such walls. The energy of such a wall as a function of the perpendicular field was determined in[140].

By using an electron microscope, it is possible to measure the width of the domain walls. Experimental data on the width of the wall (2a) makes it possible to determine the exchange-energy constant A, if one knows the uniaxial anisotropy constant K_u. If one uses the law obtained for the variation of the magnetization angle of the wall by taking into account only the exchange energy and the anisotropy energy[141],

$$\cos\theta = \operatorname{th}\xi/\delta, \qquad (6)$$

where ξ is the coordinate perpendicular to the wall ($\xi = 0$ corresponds to the center of the wall), $\theta(\xi)$ is the angle between the magnetization and the plane of the film for Bloch walls and the angle between the magnetizations in the wall and the neighboring domain for Neel walls, and $\delta = \sqrt{A/K_u}$, then the connection between the quantities of interest to us takes the form $2a = \pi\delta = \pi\sqrt{A/K_u}$. A was determined from this relation using the experimental data on the wall width[98,142,143]. Measurements performed on an Ni film (2a = 550 Å) yielded the value $A \approx 0.5 \times 10^{-6}$ erg cm; the values of A were also obtained for different Cu contents. The value $A = 0.8 \times 10^{-6}$ erg/cm obtained for permalloy[144] is in good agreement with the data obtained by other methods.

2. Wall image contrast in the defocused media. The expressions for the contrast K(x) of the boundary image in the defocused mode, for a point electron source, are obtained by substituting the corresponding function of the change of the magnetization in the wall in expressions (2) and (3). The difference between the approaches from the points of view of wave optics (2) and geometrical optics (3) are particularly strongly pronounced for a converging wall[145], where at sufficiently small illumination aperture (2β) the expressions (3) give a result that is utterly incorrect.

At $2\beta \leq \lambda(Z + S)/4ZS\gamma_\xi$, interference fringes are observed on the image of the converging wall; this was first observed in[18]. It follows from (2) that the distance between the interference fringes is $\Delta x_f = \lambda(Z + S)/2S\gamma_\xi$, the width of the fringes referred to the plane of the sample is equal to $\Delta\xi_f = h/2deB_\eta$, and the flux through the section of the film between ξ and $\xi + \Delta\xi_f$ is Φ_0. With increasing Z on the image of the converging wall, the number of fringes increases as well as their width, but the fringe width $\Delta\xi_f$ referred to the plane of the film remains the same[87].

Figure 10 shows a photograph of a domain wall with cross ties that serve as the converging sections of the wall. The small illumination aperture has made it possible to obtain a very sharp picture of the interference fringes.

Whereas for a converging wall the difference between the results obtained with the aid of wave optics and geometrical optics is large, for a diverging wall this difference is much smaller. By way of an example we

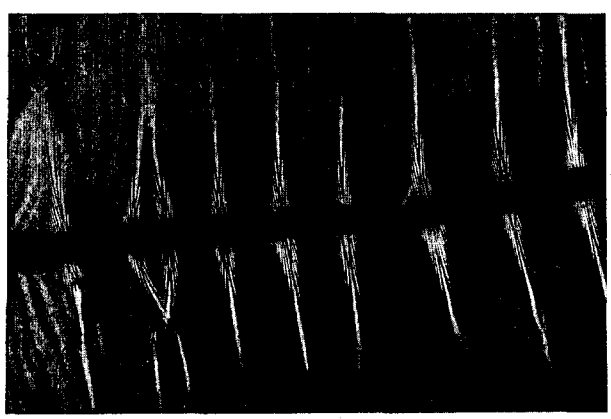

FIG. 10. Micrograph of a wall with cross ties, obtained at a small illumination aperture. Ni-Fe film, d = 500 Å, Z = 3 cm (R. H. Wade, unpublished photograph).

present a comparison for a wall of zero width[68]: $M_\eta = M_S$ for $\xi > 0$ and $M_\eta = -M_S$ for $\xi < 0$. From (1) we have $\Delta\varphi = A_0|\xi|$, where $A_0 = 4\pi M_S ed/c\hbar$, and from (2) we have

$$U_\pm(x) = A\left[\frac{\pi ZS}{k(Z+S)}\right]^{1/2}\{\exp i[k(Z+S)+\theta_\pm]\}\left\{\left[\frac{1}{2}+C(\sigma_\pm)\right] + i\left[\frac{1}{2}+S(\sigma_\pm)\right]\right\}. \quad (7)$$

where

$$\sigma_\pm = \left[\frac{kSZ}{\pi(Z+S)}\right]^{1/2}\left(\pm\frac{x}{Z}-\frac{A_0}{k}\right),$$
$$\theta_\pm = \frac{k}{2Z}\left[x^2-\frac{Z^2S}{Z+S}\left(\frac{x}{Z}\pm\frac{A_0}{k}\right)\right].$$

$C(\sigma)$ and $S(\sigma)$ are Fresnel integrals, and the plus and minus signs of $U_\pm$ denote integration over the region $0 < \xi < \infty$ and $-\infty < \xi < 0$, respectively. Recognizing that $|u_0|^2 = 2\pi ZSA^2/k(Z+S)$ and that at large $\gamma_0 Z$ the contribution from negative ξ to the region $x > 0$ is small, we obtain for the contrast ($x > 0$) the following expression:

$$K(x) \approx \frac{1}{2}\left\{\left[\frac{1}{2}+C(\sigma_+)\right]^2+\left[\frac{1}{2}+S(\sigma_+)\right]^2\right\}. \quad (8)$$

This is the contrast for diffraction from a half-plane $-\infty < \xi < \gamma_0 Z$. In Fig. 11 this dependence is represented by the solid line, and the dashed line represents the contrast obtained from (3). We see that the kinks present in the geometrical contrast are smoothed out in the diffraction contrast.

If the changes in the positions of the magnetization in the wall are smooth, the difference becomes even smaller. Numerical calculations of the image contrast of the converging and diverging walls with distribution of the magnetization in accordance with (6) have shown that for a diverging wall geometrical optics remains suitable for the calculation of the contrast even in the case of large degrees of defocusing[90], and not only in the case $Z < (d\gamma/d\xi)^{-1}$[146,147]. The condition for the validity of geometrical optics (4), obtained using the stationary-phase method (an estimate of this method is given in[148]) shows that for converging walls, corresponding to $B'(\xi) < 0$, the condition for the limitation of Z is more stringent than for diverging walls, for which $B'(\xi) > 0$. Therefore the limitation obtained for converging walls $Z \ll (d\gamma/d\xi)^{-1}$[149] is too stringent for diverging ones, and for the latter geometrical optics turns out to be valid for large values of the defocusing Z.

a) Finite dimension of electron source. Formulas (2) and (3) for the contrast K(x) were obtained under the condition that the electron source is point-like. A real electron source always has finite dimensions. This leads to a modification of the contrast, which can be written in the form of a convolution of the function K(x) with a source function f(u):

$$K_1(x) = A\int_{-\infty}^{+\infty} K(u+x)f(u)\,du, \quad (9)$$

where $u = \beta Z$. For a round source with a brightness that is constant within the limit of the angle $\pm\beta_0$ we have $f(u) = [(Z\beta_0)^2 - u^2]^{1/2}$[150], and for a source with Gaussian angular distribution $f(u) = \exp(-u^2/Z^2\beta^2)$[145]. In most cases, with the exception of the case when small condenser diaphragms are used for strong cutoff of the beam, the electron source has a Gaussian distribution.

The image contrast curves of domain walls with different magnetization distributions, at different illumination apertures, are given in[145,150-152]. The finite dimensions of the source lead to a smoothing of the contrast (the intensity of the converging walls decreases, and that of the diverging ones increases), and this effect is stronger the larger the defocusing and the illumination aperture. Calculations show that the difference between the results obtained with the aid of geometrical and wave optics decreases with increasing illumination aperture. Thus, at $2\beta \approx 10^{-5}$ rad, the oscillations on the wall boundary image vanished for films with parameters d = 500 Å, 2a = 500 Å and d = 200 Å, 2a = 800 Å, and with further increase of the aperture the similarity between the diffraction contrast and the geometrical contrast increased.

In[150,153] is given the dependence of the contrast at the center of the image of a wall with a magnetization distribution in accordance with (6) on the value of the defocusing for both types of source function. The parameter employed was the quantity β/γ_0.

b) Scattering of electrons in film. We considered earlier the contrast due only to the magnetic structure, neglecting the scattering of the electrons in the film. Actually, elastic and inelastic scattering of the electrons can take place in the film, and this changes the contrast due to the magnetic structure. Electrons scattered through angles θ that are larger than the diaphragm aperture of the objective lens (θ_0) will be blocked by the diaphragm. Electrons scattered through angles $\theta < \theta_0$ will fall into the image and produce a relative background $I/I_0 = \exp(-Qd)$, where Q is the total cross section for the scattering of the object. For polycrystalline films of Fe, Ni, Co, and Ni-Fe, one can use for Q, with good accuracy, the data obtained for an amorphous germanium film[154].

To determine the contrast it is necessary to take into account the angular distribution of the electrons scattered through the angle $\theta < \theta_0$. Since the wall is a one-dimensional object, it is expedient to use the one-dimensional distribution function $G(\theta) = (dI/d\theta)I_0$ (the intensity of scattering into a narrow slit of width $d\theta$). The contrast of the wall image is then written in the form[153]

$$K_2(x) = \frac{1}{T}\int_{-\theta_0}^{+\theta_0} K(x-\theta Z)G(\theta)\,d\theta. \quad (10)$$

It is difficult to calculate the function $G(\theta)$ theoretically, for at angles $\theta < 10^{-4}$ rad the main contribution is

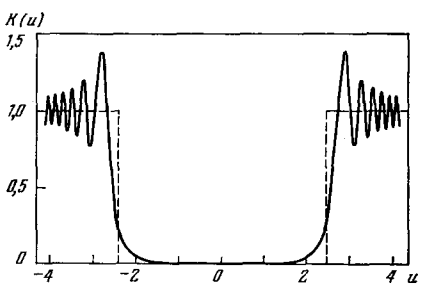

FIG. 11. Contrast of image of diverging wall, calculated with the aid of wave optics (continuous line) and geometrical optics (dashed line) for 2a = 0, d = 500 Å, M_S = 800 G, S = 20 cm, and Z = 5 cm [68].

made by multiple scattering. It can be measured experimentally by using the pattern of small-angle electron diffraction.

With increasing accelerating voltage, both the electron scattering and the deflection γ_0 in the magnetic field decrease. However, as shown in[155-157], the decrease of the scattering predominates. Under ordinary working conditions, the contrast increases with increasing accelerating voltage and reaches a flat maximum in the interval 400–700 kV. Investigations of Ni-Fe films of thickness 1500–2000 Å at accelerating voltages 200–650 kV have confirmed the predicted growth of the contrast. In these measurements, the background of the inelastically scattered electrons was subtracted (the black level was chosen to be, just as in[44], the intensity on the image of a grid).

c) Influence of character of the magnetic structure on the contrast of the walls. The presence of a regular domain structure, at sufficiently large defocusings, can distort the contrast from the domain walls[91]. In this case, the domain structure acts like a diffraction grating. Thus, for the regular domain structure of $CrBr_3$, the contrast in the case of strong defocusing approaches sinusoidal. At small values of the defocusing, when the action of the regular domain structure can be neglected, the contrast is well described by wave optics, while geometrical optics gives an incorrect result, even with respect to the magnitude of the contrast at the center of the domain wall (the condition (4) is apparently not satisfied). It is interesting that in a comparison of the diffraction contrast for 2a = 0 and 2a = 56 Å (this value was taken from the data of[158], where it is not stated how this quantity was measured), the value of the contrast at the center of the wall remained practically unchanged, so that it is hardly possible to determine the wall width from the contrast under these conditions. A similar case apparently takes place also for cementite (Fe_3C)[159], where a wall width of 100 Å was obtained for samples 2000 Å thick.

Distortion of the wall image contrast as a result of the action of the periodic magnetic structure was observed for Co and was calculated theoretically. If the magnetization in the neighboring domains goes out of the plane of the film, then the image contrast of a single wall is an asymmetrical function. This was qualitatively confirmed experimentally for walls of the basal plane[160].

3. Boundary image contrast in other microscope operating modes. a) Ray-intercept Method. The factors limiting the accuracy are as follows: 1) the finite dimension of the electron source, 2) the increase of the spherical aberrations as a result of the shift of the aperture diaphragm, 3) astigmatism due to contamination of the diaphragm, 4) inelastic scattering of the electrons, and 5) inaccurate setting of the diaphragm in the rear focal plane of the objective. The deterioration of the resolution due to the shift of the diaphragm can be decreased by placing the knife edge in the projector[24].

At a sufficiently small illumination aperture, interference fringes parallel to the domain wall are obtained on the image. The contrast from a wall of zero width was considered in[87], where a number of singularities was revealed (in particular, one interference fringe in this regime corresponds to a flux $2\Phi_0$). In the case of a small value of B_η ($CrBr_3$)[91], no interference fringes are observed on the image and the region of the transition from the light to the dark sections depends little on the width of the domain walls.

Owing to the difficulty in monitoring the location of the diaphragm that produces the contrast, and also owing to the more complicated calculation of the contrast, the cutoff method is difficult to employ for quantitative investigations.

b) Method of quarter-wave plate and interference microscopy. These methods are difficult to realize and offer no advantages whatever over the defocusing method.

c) Method of small-angle electron diffraction. It is difficult to obtain information on the domain wall in investigations of periodic magnetic structures by this method[78,69]. A difference in the wall width can lead to double spots, which can take place also when the domain widths are different[69]. However, to determine the wall structure one can use small-angle diffraction from a small region of the film, containing a single wall. The diffraction images of several sections of the walls are shown in Fig. 12. A smooth rotation of the magnetization in the wall causes lines joining diffraction spots to appear on the image[78,69]. Patterns with both straight and bent links were observed experimentally[118], although a theoretical analysis shows that the images of the Neel and Bloch walls have the same configuration, for in either case the diffraction spots are joined by a straight line (there is no displacement of the electrons along the boundary to cause the bending of the link).

In the case of small-angle diffraction, the image can be regarded as a diagram showing the distribution of the magnetization[161]. This was used in[162], where a new model of the domain wall was proposed, and in[385], where the residual magnetization of Co-P films was determined.

4. Methods of determining the width of the wall and of the course of the magnetization in it. At the present time there is abundant experimental material obtained by measuring the width of the domain walls (see the table). However, the fact that these data were obtained by different methods makes it sometimes difficult to compare the results of different authors. In addition, when measuring the wall width it is always necessary to determine whether there is a magnetostatic charge on the wall, for if the wall is charged the field of the char-

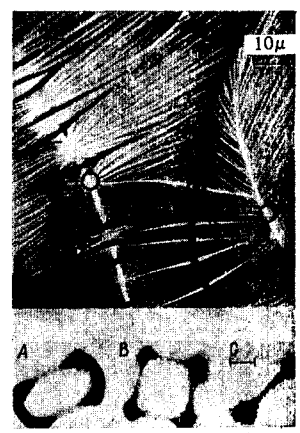

FIG. 12. Walls with cross ties and diffraction images from round regions (A, B, C). Scale–2.5 × 10^{-5} rad [69].

ges can act like an additional lens and change the value of the defocusing[38,381].

a) Method of selecting the distribution parameter. In this method one uses a certain one-parameter distribution of the wall magnetization (most frequently (6)), and the value of the parameter is chosen such that the theoretically calculated contrast approximates in best fashion the experimentally obtained one. This method was proposed in[40], where the two parameters R and δ were selected, and expression (3) was fitted to the experimental data obtained by photometry of the negatives.

This method was used to measure the wall width in films of permalloy and Co in a wide range of thicknesses[146,147]. Small defocusings were used ($Z \ll (d\gamma/d\xi)^{-1}$, and the measurements were made on the diverging walls. The dependence of the wall width on the thickness, for a film of 76% Ni-Fe is shown in Fig. 13. The experiment yielded very large values of the wall widths for thick films, which did not agree with the calculation. The main source of the error, the magnitude of which increases with thickness and leads to overestimates of the domain-wall widths, is the decrease of the contrast as a result of electron scattering in the film. Repeated measurements with an ultra-high-voltage microscope for a Ni-Fe film 1500 Å thick gave wall widths one-third as large[163]. Other sources of errors were the finite dimensions of the electron source, which was not taken into account, and the use of small defocusing, the determination of which could result in an additional error[90].

The method of selecting the parameter itself can lead to considerable errors if the employed distribution

Table showing results of measurements of domain walls (see[384])

Measurement method	Chemical composition of film	Film thickness, A	Angle of rotation magnetization in the wall, deg	Width of wall, A	Reference	Remarks
Method of selecting the distribution parameter	50% Ni—Fe	200	100	1500	40	
	76% Ni—Fe	200—1800	180	6000—2000—9000	146	Fig. 13
	Ni—Fe	1500	180	1570	167	
			140	2820		
			70	3080		
			90	3760		
	Co	200—1500	180	4000—3000—6000	147	
	Fe, Si—Fe (100)	500—1000	90 and 180	Results are different when different distribution functions are used	164	Width of 90° and 180° walls in Si-Fe increases with thickness
	Fe (100)	—	180	1720	165	
			90	770		
	Fe—Si		180	2530		
			90	1140		
From contrast at the center of the wall image	Co	—	180	150—180	150	
	Ni—Fe	1500	180, 140, 90, 70	Agreement with the selection method	167	
Method of half-difference and extrapolation to zero defocusing	Fe	1500—2000	—	1400	56	
	Ni—Fe	200	—	1800±500	168	
	Ni	200	—	550±150		
	Fe	200	—	1000±400		
	Fe epitax	700	90and180	900and1800	169	In [170] the measurements were made on the same films of thickness 400—800 A. No dependence of the wall width on the thickness was observed
	Ni epitax	350	90and180	350and750		
	β-Co epitax	950	90and180	700and1250		
	Co	100—300	180	800—900	171	
	Ni—Fe	120—530	30—160	Puc. 9	117	
	Fe	200	180	500	173	
	Ni	200	180	600		
	20—86% Ni—Fe	200	180	550—1200—750		
	Fe	170—760	180	700—500—650	145	
	76% Ni—Fe	1500	180	900	163	The value at Z = 0 is given
			170	500		
			140	130		
	Fe	100—800	Walls with cross ties	400	175	Values at Z = 0 are given, to obtain the wall width it is necessary to separate by 0.56 or by 0.66, depending on the type of boundary. The best agreement with Hubert's method
	Ni	200—600		400—500		
	Co	200—800		800—600		
Fuchs' method	81% Ni—Fe	100—800	180	7000—1000	26	Fig. 13
Inversion method	79% Ni—Fe	100—430	120	3500—1200	44, 178	Fig. 13
	Ni—Fe	100—500	180	—	180	Large scatter of points
Ray intercept method	Fe	—	90	1000±300	181	Good agreement with theory
	Ni	—	70.5	450±150		
	Ni—Co	—	60	2000±500		
	Co	—	180	200±50		
	Magnetoplumbite crystal	2000	—	250±150	182	
	Co crystal	—	—	500±100	183	

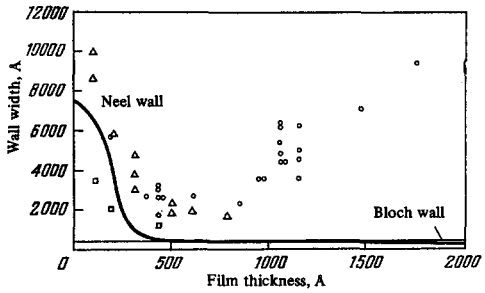

FIG. 13. Width of 180° domain wall as a function of the film thickness for 76% Ni-Fe. Continuous line-calculation in accordance with [96], Δ–data of [26], O–[146], □–[44] (120° wall in film of 79% Ni-Fe).

of M_S differs from the real one, and the error itself cannot be controlled. This was confirmed by the data of[164], where the wave-optics formulas were used to calculate the contrast for certain distributions of the magnetization in the wall and a comparison was made between the theoretical and experimentally obtained contrasts for samples of thickness up to 500–1000 Å polycrystalline samples of Fe and Si-Fe). The values of the wall widths determined using different distributions differed quite appreciably.

b) Method of determining the wall width from the contrast at the center of the wall image. This method was proposed[150] for a magnetization distribution in the wall in accordance with (6). The expression for the contrast at the center of the image of a diverging wall is $K(0) = [1 + RS(Z + S)^{-1}]^{-1}$. From this expression, knowing the value of the defocusing and the angle of inclination of the electrons in the neighboring domains (from the splitting of the diffraction spots in diffraction of the electrons by the wall and the adjacent regions of the neighboring domains[25], and knowing the film thickness, it is possible to determine also M_S[166]), it is possible to determine the parameter δ and the wall width.

With such a determination of the wall width, it is easier to take into account the finite dimension of the source, and K(0) can be determined at rather large defocusings. A comparison of the geometrical contrast with the wave-optical one[90] has shown that $K(0)_{geom} = K(0)_{wave}$ even at large Z (~5 cm), whereas the differences between the values of K(x) on the edges limit the utilization of the selection method. In determining the wall width by this method, the greatest error is introduced by the electron scattering in the film and the resultant decrease in the contrast. The error due to the scattering of the electrons in the film is approximately the same in this method as in the preceding one. It is interesting that both methods give close values of the domain-wall width[167].

c) The method of half-sum or half-difference. This simple method was proposed in[56] and was subsequently developed in[168,144]. The calculation was carried out with the aid of geometrical optics. The width of the image of a diverging wall in the observation plane is $W_d = ((Z + S)/S)2a + 2Z\gamma_\xi$ and that of a converging wall is $W_c = ((Z + S)/S)2a - 2Z\gamma_\xi$ for $((Z + S)/S)a > Z\gamma_\xi$ and $W_c = 2Z\gamma_\xi - ((Z + S)/S)2a$ for $((Z + S)/S)a < Z\gamma_\xi$. The width of the wall is obtained as the half-sum or half-difference of the widths of the images of the diverging and converging walls in the observation plane. The value of the defocusing is preferably made large, for in this case the distribution of the contrast is close to rectangular and it is easier to determine the edge of the wall. As seen from the expressions, when determining the width of the wall it is necessary to take into account the coefficient S/(Z + S), for otherwise the obtained values of the wall widths will be too high. This method was used in[56,117,145,168,173,382] to obtain the values of the wall listed in the table.

This method is simple but has many shortcomings:

1) A small quantity is determined as a difference of two large ones, which can lead to a large error.

2) When the width of the image is measured at some definite level of the contrast, different results are obtained for different models of the walls[144].

3) To reduce the error it is necessary to introduce correction coefficients[144] that depend, however, not only on the thickness of the film and the wall width, but also on the illumination aperture and on the distribution of the magnetization in the wall[145].

4) Whereas geometrical optics is suitable for the description of the contrast of diverging walls, it introduces considerable errors in the case of the converging walls[145].

5) In the measurements it is also necessary to take into account the fact that the film density can be lower than that of the bulk material[77,144] (according to other data[174,166] this was not observed).

The error is smaller in the method of determining the wall width only from the image of a diverging wall with extrapolation of the half-width of its image at the 1/2 level to Z = 0[145,153,175,125]. The wall width measured in this manner corresponds to the distance, in the wall, between the points of which $|dB/d\xi| = 1/2$. The result of the measurements by this method depends little on the finite dimensions of the illumination source, on the use of the geometrical-optics relations, and of small-angle scattering of electrons in the film. The latter has an even smaller influence than the finite illumination aperture[153,175]. Recent measurements[372] gave results that agreed well with the theoretical ones calculated in accordance with the model of[107]. However, it is precisely for this model, as shown in[373], that this method results in errors by a factor of 3.

d) The Fuchs method. This method was first used to attempt to determine the course of the magnetization in a wall[49,26]. In this method it is necessary to determine the distance between the maxima of the intensity on the image of a converging wall. Since the calculation is based on geometrical optics, and it was shown in[176] that the maxima on the diffraction pattern lie far from the caustics calculated with the aid of geometrical optics, this leads to considerable errors (the width is overestimated by more than 2 times[20]).

The results of the investigation[49] indicated the presence of two regions in a Neel wall: 1) region of strong variation of the direction of the magnetization, and 2) region of slow rotation of magnetization. The appearance of the regions of slow rotation is connected with the stray fields of the Neel wall. Theoretical calculations also lead to the presence of such regions[99]. The regions of slow rotation are much broader than the region of fast rotation: thus, slow rotation occurs in a

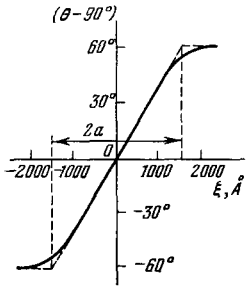

FIG. 14. Change of the angle of rotation of the magnetization in a 120° boundary of a film 79% Ni-Fe of 100 Å thickness [44].

region of width 10—15 μ, whereas the width of the narrow region is ~0.1 μ[107].

e) Inversion method. This method makes it possible to determine the course of magnetization in the wall[44,178-180] and to obtain the absolute value of M_S. The inversion can be carried out graphically or analytically. In the first case, the magnetization component parallel to the wall is equal to

$$M_\eta(\xi) = \frac{\sqrt{U_0}}{\pi\sqrt{8e/m}\,Zd}\Delta x(\xi), \qquad (11)$$

where $\Delta x(\xi)$ is the displacement of the electron trajectories in the observation plane. The displacement is determined from integral curves obtained by integrating the current density on the image of a diverging wall, and M_η is determined from (11). The obtained $\theta(\xi)$ plot is close to linear (Fig. 14). The absolute value of the wall width decreases with increasing film thickness much less than in[26] and[146] (see Fig. 13). The obtained absolute value of M_S was close to the magnetization of bulk material (~800 G), and no decrease in the film density in comparison with the bulk material was noted.

Analytic inversion[179,180] gives for M_η the expression:

$$M_\eta(\xi) = M_S\sin\theta(\xi) = \frac{M_S k(Z-S)}{2ZSA_0}\int_{-\infty}^{+\infty}[1-K(x')]\,\mathrm{sgn}(x-x')\,dx', \qquad (12)$$

$$\xi = \frac{S}{Z+S}\left[x - \frac{ZA_0}{k}\sin\theta(\xi)\right],$$

where $A_0 = 4\pi M_S ed/c\hbar$.

Calculation of the function $\theta(\xi)$ was carried out with a computer, using the contrast curves obtained by photometry of the image of a diverging wall on the negative. Measurement of the wall width was carried out on permalloy films of thickness 100—800 Å.

When using the inversion method, it is also necessary to introduce a correction for the background of the inelastically scattered electrons. In the general case it is difficult to take into account the small-angle scattering of the electrons[153]. For films of thickness ~500 Å, however, its contribution is small. The main errors for films with these thicknesses are due to the finite dimensions of the electron source and due to the use of the geometrical methods in the calculations. These errors increase with increasing defocusing Z. However, an estimate of these errors[151,152,180] has shown that the method has sufficiently high accuracy under real operating conditions in the case of a sufficiently strong contrast (small defocusing and accordingly weak contrast are practically unusable, owing to the small signal/noise ratio). This, the use of medium defocusings ($Z \leq 5$ mm) gives in most cases an accuracy of $\theta(\xi)$ not worse than 10°[180].

f) Methods using wave-optics calculations. The expressions obtained with the aid of wave optics for the contrast are complicated and do not make it possible to determine $\theta(\xi)$. The method of selecting the parameter[20,68,160,164] has the same shortcomings as when it is used with the geometrical-optics expressions. For Co, however, this method yielded good quantitative agreement for the image contrast of converging walls in the prismatic plane[160]. Although in this case the error can also be quite large, owing to inaccurate knowledge of the dimensions of the source (this was noted in[373], where methods of measuring wall widths are compared), the measured wall width agreed with the data by other authors.

g) Ray intercept method. In[23,24], an attempt was made to obtain data on the boundary by measuring the distribution of the intensity across the image of the boundary while moving the edge of the diaphragm. A strong influence of the unevenness of the diaphragm edges was noticed in this case. When converging illumination is used[181] (the line joining the diffraction spots became blurred[25]), the intensity of the electrons passing through each element of the wall is proportional to the magnetization component parallel to the wall. In the experiment, the convergence of the illuminating electron flux was increased until a constant intensity profile of the wall was obtained, which was then compared with the theoretical one corresponding to the distribution of the magnetization in accordance with (6). The data on the wall width were given in the table.

The intercept method was used also to determine the wall width in the basal plane of thin uniaxial crystals with high anisotropy (Co, magnetoplumbite), where the magnetization in the domains is almost perpendicular to the surface of the sample, and the magnetization in the walls becomes parallel to the surface[181,182] (see the table). In this case the diffraction spot does not become split, but acquires wedge-like stubs. If the aperture diaphragm cuts off one of the stubs, then the walls on the image take the form of dark and bright lines against the background of domains with equal illumination, and the widths of these lines correspond to the wall widths. For Co, the walls are seen very distinctly (Fig. 15).

The errors in the intercept method were noted earlier in the analysis of the contrast from the domain walls.

IV. FINE STRUCTURE OF MAGNETIZATION INSIDE DOMAINS (MAGNETIZATION RIPPLE)

1. Contrast of magnetization ripple. The quasi-periodic oscillations of the magnetization inside domains (the magnetization ripple; see Fig. 12) were observed in[21,40,36,184,63,185], and it was shown that out of the two models, namely longitudinal oscillations of the magnetization (along the average direction of magnetization) and transverse ones, the former is more favored energywise and gives a larger contrast in the defocusing mode. The ripple line on the image is perpendicular to the local direction of magnetization, and this was used to investigate the behavior of the magnetization near defects, inclusions, and cavities in films[186,24,182,187]. The possibility of determining the relief of the films from the ripple lines was also demonstrated[188].

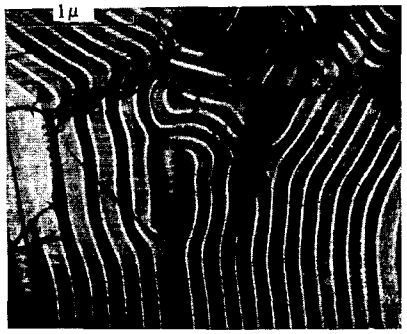

FIG. 15. Image of domain structure in a single crystal of Co (0001) in the ray intercept mode [183]).

The sources of ripple are inhomogeneities in the film, which lead to changes in the local anisotropy both in magnitude and in direction. The presence of magnetization oscillations affects the macroscopic properties of the film. These questions are considered in detail in the reviews[189,190].

Theories of magnetization ripple were developed in order to obtain relations between the magnetic properties of the sample and the parameters of its real structure[191-196]. In addition to a linear theory[193,194], there has been developed by now a more general nonlinear theory of ripple[195,196].

The characteristics of the ripple are the amplitudes and wavelengths of the harmonics. According to the linear theory, the dominant oscillations are those with the wavelength

$$\Lambda_{LR} = 2\pi \sqrt{A/K_u h(\alpha)}, \qquad (13)$$

where $h(\alpha) = h\cos(\alpha - \varphi_0) + \cos 2\varphi_0$, $h = H/H_k = HM_S/2K_u$, H is the intensity of the external field applied at an angle α to the easy-magnetization axis, φ_0 is the angle between the average direction of the magnetization and the easy axis, Λ_{LR} is the fundamental wavelength of the ripple along the average direction of the magnetization, and K_u is the uniaxial anisotropy constant (knowing Λ_{LR} from expression (13), we can determine A[197]). Another pronounced oscillation, of short wavelength with wavelength $\Lambda_{SR} = 4D$, is determined by the average dimension of the crystallites D and coincides with the result of[191].

The experimental investigations of the fine magnetic structure were aimed either at verifying the validity of the theoretical results, or at establishing the causes of random anisotropy. In many cases, the linear theory agreed sufficiently well with experiment (e.g., the depencence of Λ_{LR} on the field along the easy and difficult axes[194,198-201]), and in others there was no agreement (the dependence of the angular dispersion on the dimension of the crystallites[202,203]). In some cases good agreement with experiment was obtained by the simple theory of[191] (dependence of Λ on the dimensions of the crystallites[204]).

At the present time, only transmission electron microscopy makes it possible to observe magnetization ripple. When considering the contrast of the magnetization ripple, it is necessary to use wave optics.[87] Geometrical optics results in a direct proportionality of the dependence of the contrast on the frequency of the harmonic of the ripple, whereas wave optics yields an inverse proportionality (the contrast of the higher harmonics becomes smoothed out). This smoothing is clearly seen in Fig. 16, which shows for comparison the contrast from different models of the ripple for the same change of the flux $\Delta\Phi_r = 4\pi M_S \theta_0 \Lambda d$, where θ_0 is the amplitude of the angular deviation and Λ is the wavelength. The geometrical contrast approximates well the wave-optical contrast only in the first case. The suppression of the higher harmonics can be explained qualitatively also on the basis of geometrical optics[199]. Indeed, if $\Lambda < 2Z\gamma_r$ (γ_r is the angle of deflection as a result of the magnetization component perpendicular to the average direction of magnetization), then the images of the neighboring periods of the ripple become superimposed on one another and the contrast becomes smeared out. Long wave oscillations ($\Lambda > 2Z\gamma_r$) have a weak contrast. A microscope in the defocused mode thus acts like a band filter (as first noted in[205]), and gives the image of the ripple only with wavelength $\Lambda \approx 2Z\gamma_r$.

In the defocusing mode, when the angular deviation is $\theta \ll 1$ and the phase shift (1) due to the action of the ripple is small, wave optics yields the following expression for the contrast[206]:

$$I(x) = 1 - i\frac{2edB_S}{\hbar}\int_{-\infty}^{+\infty}\frac{\theta(\omega)}{\omega}\sin\left(\frac{Z\omega^2}{2k}\right)e^{-i\omega x}\,d\omega, \qquad (14)$$

where $\theta(\omega)$ is the Fourier transform of $\theta(\xi)$ and ω is the spatial frequency. From this relation we easily obtain $\theta(\omega)$:

$$\theta(\omega) = -i\frac{\omega\hbar}{4\pi edB_S\sin\left(\frac{Z\omega^2}{2k}\right)}\int_{-\infty}^{+\infty}[1 - I(x)]\,e^{i\omega x}\,dx. \qquad (15)$$

When deriving this relation, no account was taken of the finite illumination aperture and of the electron scattering in the film, which lead to errors in the determination of $\theta(\omega)$[207].

In Fraunhofer diffraction, the intensity on the image is proportional $(\theta(\omega)/\omega)^2$ for $\omega = \pm kx/Z$, i.e., the spatial frequency ω gives a diffraction maximum at an angle $\kappa = \omega/k$[208]. This spatial harmonics will be represented with maximum contrast if the phase shift corresponding to it is equal to $2(m-1)\pi/2$, i.e., $Z\omega^2_{max}/2k = (2m-1)\pi/2$. These spatial frequencies give in the

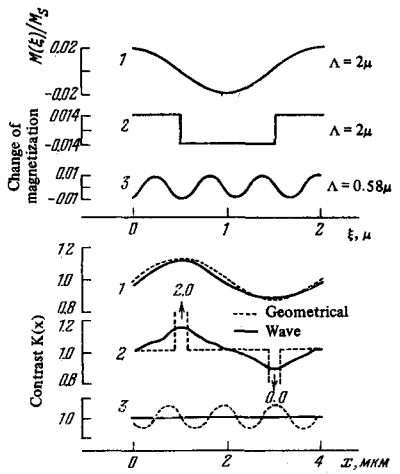

FIG. 16. Models of magnetization ripple and contrast of defocused image at $4\pi M_S$ = 10 000 G, d = 250 Å, and S = Z = 15 cm [87].

Fraunhofer diffraction mode, upon illumination by a laser of wavelength Λ_L, diffraction maxima at angles

$$\varkappa_{max} = \frac{\Lambda_\pi}{M}\sqrt{\frac{(2n-1)k}{4\pi Z}},$$

where M is the magnification of the photographic plate. The diffraction maxima of the magnetization ripple spectrum were observed in[209]. The relation for $\varkappa_{max}$ can be used to determine the magnitude of the defocusing[153,209]. Other methods of finding the working parameters of the microscope have been proposed in[210]. In[211], for sinusoidal ripple, expressions were obtained for the contrast in the Fraunhofer diffraction mode, and estimates were made of the influence of the finite illumination aperture and the small-angle scattering.

2. Influence of film parameters on the magnetization ripple. a) Dependence on the external magnetic field. In[194,201], to verify formula (13), an investigation was made of the dependence of Λ_{LR} on the external field. Wave and geometrical optics yield the same value of the wavelength on the image, and their difference is manifest only by the relative contrast of the corresponding oscillations. The results of microphotometry cannot be used to determine Λ_{LR} without an additional complicated analysis, since the emphasis of the high-frequency components may separate on the image the short-wave oscillations, which are suppressed in a film as a result of the exchange forces. Λ_{LR} can be determined, however, by observing from a certain distance the magnification of the photograph or by suppressing the higher oscillations from the image with the aid of an additional alternating magnetic field applied in the same direction as the constant field[201]. Λ_{LR} was practically independent of the defocusing Z when the latter was varied within a sufficiently wide range. The defocusing, however, should not be too small, for at small values of Z the contrast of the long-wave oscillations is small and a large number of higher harmonics is present in the image. The results of the experiment agreed well with the linear theory. It was impossible, however, to give preference in accordance with these results to any particular theory, that of[181] or of[184]. Figure 17 shows data on the dependence of Λ_{LR} on the field in the easy and difficult directions.

In isotropic 81.5% Ni–18.5% Fe films, ripple with two wavelengths was observed, and the length of the long-wave oscillations depended on the field in accordance with (13), although for these films we have $K_u \approx 0$ and the theory of[194] is not suitable for them. For Fe films, there was not even agreement in the behavior of $\Lambda(H)$[199]. In later investigations[212,213], the dependence of Λ on the field along the easy axis coincided with (13). What was reduced in these investigations, however, were not the $M(\xi)$ curves, but the contrast curves $K(x)$, and furthermore without allowance for the coordinate transformation, so that these data may not correspond to the true distribution of the magnetization in the film.

b) Dependence on the macroscopic anisotropy. Regardless of the cause of the local anisotropy oscillations, the presence of macroscopic anisotropy leads to a decrease in the amplitude of the ripple. This was verified experimentally on Ni films, which have a large magnetostriction, where the large uniaxial anisotropy was produced by tension. After a slight annealing, which relieved the stresses, the ripple appeared anew. The change of the ripple on Ni films precipitated at room temperature, which took place in subsequent annealings with increasing temperature, was attributed to the interaction of the external and internal stresses[199]. When Ni-Fe films with crystallite dimensions D = 80–100 Å were subjected to tension, the appearance of new anisotropy prior to the vanishing of the ripple was observed[214], unlike in films with D = 250–300 Å.

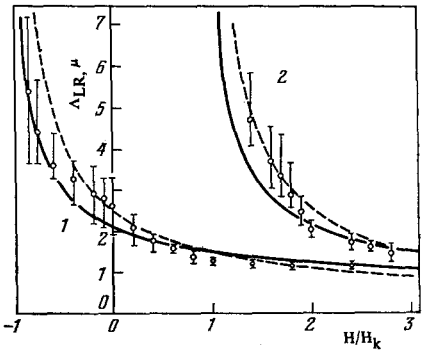

FIG. 17. Dependence of the fundamental wavelength of the magnetization ripple on the magnetic field along the easy (1) and difficult (2) axes. Film 81% Ni-Fe of 420 Å thickness [201]. Theoretical curves: solid–from [194], dashed–from [191].

For electrolytically deposited 81% Ni-Fe films (d = 500 Å), the obtained dependence of Λ_{LR} on H_k[215] was in the form $\Lambda_{LR} = 0.33\sqrt{p} + 0.2\ \mu$ for $p \leq 3.6\ \mu$, where $p = 82/H_k\ \mu$ is the distance between the ties on the wall with cross ties. This agreed with[96] and (13), but the plot did not go through the origin. In films subjected to low-temperature annealing ($t < 250°C$, i.e., when the dimension of the crystallites remained unchanged) and to high-temperature annealing ($t = 300–500°C$, the crystallites noticeably increased in size), Λ_{LR} increased only after the first few cycles. Subsequently, in spite of the decrease of H_k, the value of Λ_{LR} remained constant. This can be attributed to the fact that not all the H_k are determined by macroscopic causes (e.g., external stresses, which are relieved after weak annealing). That part of H_k which is determined by microscopic factors, although it does decrease upon subsequent annealing, does not change the value of Λ_{LR} (e.g., disordering of defects or of atomic pairs).

c) Dependence on the composition of the films. The dependence of the ripple on the composition of the films was investigated mainly for permalloy films[184,200,216-218]. A slight ripple was observed in films of composition 70–80% Ni-Fe. The ripple disappeared in 74% Ni[184,216], where the magnetocrystalline anisotropy was equal to zero for the bulk material (free standing annealed films with internal stresses relieved were investigated in[216]). In other cases[217], $\alpha_{90°}$ was minimal near the composition with zero magnetostriction (the investigated films were deposited on glass at room temperature). No dependence of Λ_{LR} on the composition (50–90% Ni) was obtained[201]. In Ni-Co films, no pronounced dependence of the ripple on the composition was observed.

d) Dependence on the grain dimension and orientation. For permalloy films obtained by deposition on

glass substrates[202,203], the dependences of $\alpha_{90°}$ on the grain dimensions did not agree with the data of[194], and the value of $K_0\alpha_{90°}$ hardly varied with the grain dimensions. Measurement of Λ[204] for fully polycrystalline films with grain dimension $D \leq 2000$ Å gave good agreement with the data of[191]: $\Lambda = 4D$, and the value of Λ remained constant at $D > 2000$ Å. For oriented films, Λ was independent of the crystallite dimensions at $D \geq 1200$ Å. However, the data of[191] do not agree with the data on perfect single-crystal films (there was no ripple) and on oriented films ($\Lambda = 10D$). A general tendency of Λ to increase with increasing D was observed also in[38,219] on 81% Ni-Fe films. For polycrystalline films of Ni, Fe, and Co, there was also observed[220] a linear dependence of Λ on D, namely, an increase of the crystallites from 300 to 700 Å changed Λ from 0.5 to 2 μ. The following should be noted here: some authors measured the wavelength of the short-wave oscillations, Λ_{SR}, and others the wavelength of the long-wave oscillations, Λ_{LR}, which is more difficult to determine from photographs. In general Λ_{SR} is proportional to the size D of the crystallites within a certain definite range $D_0 \leq D \leq D_1$. We have $\Lambda_{SR} = \Lambda_{LR}$ for $D > D_1$, and Λ_{LR} is independent of the crystallite dimensions for $D_1 \leq D \leq D_2$. No dependence of Λ_{LR} on the crystallite dimensions was observed in[215].

The coercive force H_c and Λ_{av} in[221] are compared. For films of 50–90% Ni with Fe there was observed a linear connection between Λ_{av} and H_c. It is difficult, however, to interpret this dependence as unambiguous, since no account was taken of the influence of the change of the magnetostriction and of the anisotropy constant. For films of pure Fe, Ni, and Co, a more rigorous linear connection between H_c and Λ_{av} was observed.

Orientation of the grains leads to a decrease of the ripple as a result of the decrease of the fluctuations of the local anisotropy. In Fe films with high grain orientation, the ripple is smaller than in films without a texture[222]. In monocrystalline and epitaxial high-orientation films of the pure metals Fe and Ni, the magnetic ripple was not observed[169,223], but in Ni films it was observed upon application of an external magnetic field. The presence in the film of crystallites with double orientation may be the cause of the appearance of ripple in epitaxial films[169,224]. The inhomogeneity of the composition and the disordering of the alloy were the causes of the ripple in single-crystal Ni-Fe films, which acquired a speckled domain structure after preparation[225]. In general, the dispersion of the magnetization of epitaxial Ni-Fe films is smaller than that of polycrystalline films[226], although in[227,228] ripple was observed also in well-oriented epitaxial films. The speckled domain structure was observed also in single-crystal films of Co[229,169] (and disappeared after annealing at $t \approx 600°C$). Ripple was observed also in thinned-out single crystals of the stoichiometric alloy Ni_3Mn[230]. In the investigation of single-crystal foils of 50–85% Ni-Fe, the ripple was observed in foils obtained by chemical polishing, whereas there was no ripple in foils obtained by electric polishing[199]. The reason for this is apparently the fact that the foils obtained by chemical polishing had a very uneven surface.

e) Dependence on the film thickness. The wavelength of the oscillations remains constant when the film thickness is varied, but the local deviation of the magnetization vector from the mean value increases with decreasing thickness[38,231]. The transverse wavelength is proportional to the square root of d, which coincides with the theoretical calculations of the linear theory.

f) Temperature dependence of the ripple. As shown by investigations[199,200], the wavelength of the ripple is practically independent of the film temperature. On the other hand, the amplitude of the ripple depends strongly on the temperature. Thus, in epitaxial Fe, Ni, and Co films, in which at small thicknesses (< 300 Å) there was no ripple at low temperatures, appearance of ripple was observed upon heating to high temperatures[111]. Temperature investigations of Fe, Co, and Ni-Fe films[232-234] have shown that the ripple is minimal at temperatures 300–320° C. Such a behavior can be attributed to the temperature dependences of the magnetocrystalline anisotropy constant K_k and of the crystallite dimensions D[235], namely, at first D hardly changes with increasing T, but K_k decreases, and this leads to a decrease of the contrast of the ripple, since the contrast is determined by the product DK_k. With further increase of T, the growth of D begins to predominate over the decrease of K_k, and the ripple becomes stronger. Such an explanation is confirmed by the fact that no minimum of the ripple is observed upon cooling. Naturally, the decrease of the ripple contributes to the decrease of the local anisotropy as a result of the decrease of the stresses with increasing temperature. In other observations, to be sure, a reversible decrease of the ripple was observed on cooling from 550° C[236]. In polycrystalline Co films, two temperature maxima of the ripple were observed, namely, the ripple became stronger from 300 to 400° C as a result of the growth of the crystallites, the ripple was weakly pronounced at 500° C, and at 700° C the ripple became stronger again (and at the same time a transition of Co into the cubic phase was observed)[237]. The temperature dependence of the magnetization-ripple spectrum in films was investigated in[383].

In all films, including single-crystal ones, the ripple becomes intense near the temperature of vanishing of the domain structure (T_{dc}), for example, oriented Fe films, which had no ripple at room temperature, had a strong ripple at 620° C. After several cycles of temperature variation from room to critical, the dependence of the ripple becomes less pronounced, with the exception of the temperature region near T_{dc}[199]. Usually the temperature dependence of the ripple is more clearly pronounced for permalloy films than for Fe films. For Ni it is difficult to obtain such a dependence, owing to the low temperature T_{dc}. Final vanishing of the ripple with further heating was observed in films of thickness 500–3000 Å at a temperature below the Curie point of the given material[238].

Ripple was observed[239,240] in polycrystalline films of the alloy EuS at $T < 15°K$.

g) Dependence of the ripple on the technology of producing the films. Magnetization ripple depends strongly on the substrate temperature during the time of evaporation of the films. The ripple is large both in films obtained at low temperatures of the substrate (strong anisotropic stresses) and in films deposited on

very hot substrates (large-grain structure). The minimum ripple is obtained at substrate temperatures ~200° C[241]. However, no dependence of Λ_{LR} on the substrate temperature (–150—350° C) was obtained[201], although it was predicted by the linear theory.

A comparison of Ni films obtained at different degrees of vacuum has shown that films sputtered at low vacuum, 10^{-4} Torr (unlike films obtained at 10^{-6} Torr) had ripple, this being attributed to the appearance of oxide gaps between the crystallites and to a weakening of the exchange coupling[26]. Ripple appears also in the case of graininess of the adjacent non-magnetic copper layer separating the magnetic layers[242].

In the case of oblique sputtering of films, the sputtering angle influences the ripple as a result of a change in the uniaxial anisotropy. Investigations were made on Ni-Fe films[233] and on Ni, Fe, and Co films[243,244] sputtered at angles 0—70°. At small angles, the domain structure is irregular and has a ripple inside the domains. At large angles, the domains become equalized with increasing uniaxial anisotropy, and the ripple vanishes.

Ni-Fe films obtained in a rotating magnetic field had a strong ripple[245].

V. STATIC DOMAIN STRUCTURES

The form of the domain structure depends strongly on the crystal structure of the sample, on the composition of the sample, and on the conditions of its preparation.

1. **Single-crystal foils and epitaxial films.** In single-crystal Fe films[56] there are observed exceptionally straight domain walls. 180° walls with cross ties appeared at film thicknesses 500 Å, in accord with the theoretical calculations[224]. Epitaxial Fe films obtained on NaCl at 450° C (grain dimension ~500 Å) had a considerable dispersion of the 180° and 90° walls. After annealing at 850° C, the films became single-crystal and had mainly 90° walls[246]. In epitaxial films, a domain structure with straight walls was likewise obtained[247]. The domain structure of single-crystal films does not depend strongly on the thickness[248], namely, at d = 80—200 Å the domains have an irregular shape with 90° walls, and when the thickness is increased to 2 μ the fraction of the 180° walls increases, and at d = 2—3 μ the film has the same structure as the bulk metal. When a foil of Fe was subjected to tension[249], there was observed, in contrast to the theoretically expected motion of the 90° boundaries, motion of the 180° walls and growth of the domains with M_S directed closer to the tension axis.

For single-crystal Ni foils[250], no dependence of the domain structure on the orientation and thickness of the film was obtained, as expected as a result of the small crystallographic anisotropy. In an investigation of the domain structure as a function of the temperature[251], the easy magnetization axis changed its direction from [111] to [100] at 100—150° C. The domain structure of single-crystal Ni films deposited at low temperatures was strongly dependent on the thickness of the films[252,248]. In Ni films electrically deposited on Cu, the domain structure could not be resolved, owing to the strong inhomogeneity of the magnetization[184].

In single crystals of magnetoplumbite with d = 1000—2000 Å, a sinuous domain structure characteristic of the basal plane was observed (Fig. 15)[183]. In Co single crystals, the wall direction coincided with [0001], and a change of the structure at the grain boundaries was observed[250]. If a cubic phase was present in addition to the hexagonal phase, then the domain configuration in the first phase corresponded to the Kittel model, and 90° domains were observed in the second[253,159]. On the boundary between the phases, the direction of the domain walls changed and widge-like domains appeared and lowered the magnetostatic energy. With decreasing thickness of a Co single crystal (0001), in the thickness region 280 ± 50 Å, the appearance of walls with cross ties was observed[254], indicating that the magnetization was in the plane of the sample. At a thickness ~1000 Å, cylindrical domains of 0.1—0.5 μ diameter were observed in the basal plane. Inside these domains there was either one 180° wall or a circular distribution of the magnetization[255].

The width of the 180° domains in Co depends on the orientation of the plane of the foil relative to the crystallographic axes[255,159] and on the thickness of the sample[257,250]. The influence of the crystal orientation on the domain structure was investigated in[258-260,81,83]. The calculated values of the equilibrium widths of the domains in the magnetization direction coincided satisfactorily in them with the experimental data[260]. When account is taken of the stray fields of the domains, the agreement between the theoretical and experimental data improved[261].

In epitaxial β-Co films deposited on NaCl at 200° C, a speckled domain structure was observed in the nondemagnetized state[229]. After demagnetization, large domains appeared. The character of the change of the domain structure with changing thickness was the same as for Fe[248]. The temperature dependence of the domain structure in Co foils with thickness up to 4000 Å and with different orientations was investigated in[183,262,263,251]. The experimental and calculated (after[260]) values of the domain widths and of the magnetization direction in them agreed satisfactorily for the temperature region 20—250° C, where Co is uniaxial ($K_1 \geq 0$). The decrease of the anisotropy energy at higher temperatures and the presence of more than one easy axis, when $K_1 < 0$, explain the formation of a closing domain structure on the non-magnetic inclusions[262]. In a foil of hexagonal Co (1010), the direction of the magnetization changed to perpendicular at ~300° C, and no changes in the magnetization direction were observed for a foil of cubic Co up to 500° C[263]. For Co (0110) foils[251], the change of the direction of the easy axis with changing temperature was in good agreement with data on the change of the dependence of the anisotropy constants on t. The direction of magnetization changed to perpendicular at 535° C, and the width of the domains remained unchanged. In a Co foil with prismatic orientation, the realignment of the domain structure occurred at 330° C (Fig. 18). Figure 18 shows clearly the closing domain structure (A).

Very thin epitaxial Fe, Ni, and Co films are characterized by predominance of 90° domains[111].

In multi-axial single-crystal foils the magnetization in the domains can go out of the plane of the foil, owing

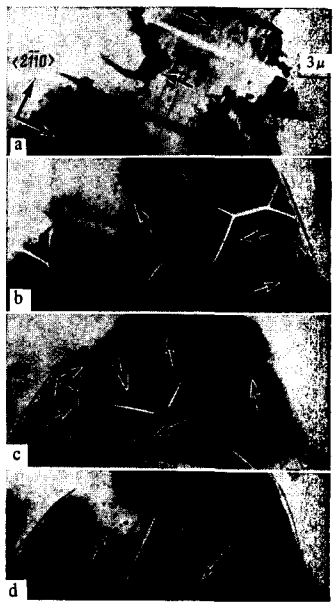

FIG. 18. Domain structure of Co foil (prismatic plane) as a function of the temperature: a) room; b) 270°C, c) 305°C, d) 330°C [251].

to the perpendicular anisotropy. This gives rise to a very regular structure, of the so-called strip domains, in which the magnetization experiences wave-like deviations from the plane of the foil. Such a strip structure was observed in Fe (111) foils of thickness larger than critical (1300—4000 Å) (Fig. 19), where a structure of strips with period ~1000 Å, parallel to the average direction of magnetization in the domains[264], was present inside the ordinary 90° domains, and also in Ni foils[265]. Apparently, the fine strip structure inside the large domains in Fe[266] is also the structure of strip domains.

The typical closing domain structure on the edges of the sample, the wedge-like and tubular domains at the holes, and bending of the domain boundaries at the holes were observed on foils of Fe[258,267,268], Ni[258], Co-Fe[187], Ni_3-Mn[269], and Co[262,251]. The equilibrium lengths of the wedges produced at the opening were calculated in[270], and sufficiently good agreement with experiment was obtained. In[271,272], electron diffraction was used to study the distribution of the magnetic charges on the edge of the Co foil. The influence of inclusions on the structure of the domains was demonstrated on films of the FeCr alloy[273]. A strong influence of the antiphase boundary on the domain wall was noted in[274]. In single-crystal Fe films, inclusions of micron dimensions lead to violation of the homogeneity of the magnetization in the domains and to the occurrence of a substructure[182]. The irregular domain structure and the bending of the wall can be due also to elastic stresses, as is the case in a completely ordered alloy 50.7% Co-Fe with large magnetostriction constant. In disordered alloys, 27.1% and 71.4% Co-Fe, where the magnetostriction does not play such a role, the domain walls are regular and the easy axis in the plane of the film is determined by the crystallographic anisotropy[187].

Attempts were made to observe the interaction of the domain walls with dislocations[250,258]. It was noted that in the case when the wall is parallel to the dislocation line, there is a certain delay in the motion of the wall.

The domain structure of single-crystal Ni-Fe films was investigated in[225]. The obtained films were either single-domain or had a speckled structure, the appearance of which is due to the imperfection of the film and to the disordered character of the alloy. After demagnetization, the single-domain films had large domains with the 90° walls along the difficult magnetization axis and 180° boundaries along the easy axis. In the speckled films, when demagnetized along the easy magnetization axis, the speckles were aligned in the ripple lines and walls made up of individual points were observed in the case of demagnetization along the difficult axis.

A domain structure of a two-layer single-crystal film with a layer of LiF was observed in[275,276,384]. The interaction of the walls in the different layers led to the formation of complicated and unusual domain walls. The domain structure of $CrBr_3$ and CrI_3 was investigated at helium temperatures[91,277]. At $A \equiv M_S^2$ the theoretical dependence of the domain width on the temperature agreed well with the experimental one. Application of a perpendicular field (2 kOe) led to the appearance of a honeycomb domain structure.

The domain structure of different alloys was investigated in[158,230,269,278,279], and that of antiferromagnets was investigated in[280-282].

2. Polycrystalline films. In the investigation of uniaxial precipitated polycrystalline films, it is necessary first of all to know the directions of the easy and difficult axes. It is easier to find the direction of the difficult axis by determining the disintegration of the structure after application and removal of a constant magnetic field.[283] In an electron microscope it is possible to obtain $\alpha_{90°}$, H_k, and H_c[283,284]. It must be recognized, however, that a rotating anisotropy appears in films removed from substrates, and can lead to incorrect values of H_k and $\alpha_{90°}$[285]. In this case, naturally, the data obtained in an electron microscope can differ for a film on a substrate and for a film without a substrate. Experiments[285] have shown that only in the case of a sufficiently thick sublayer (SiO, d > 1100 Å) is there no rotating anisotropy.

In[122] there were observed simultaneously pictures of the domains and of the crystallites in a large-crystal Ni-Fe film in which grains with dimensions up to 10 μ

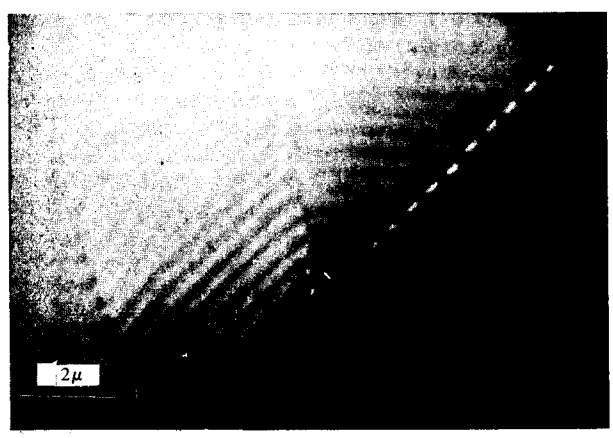

FIG. 19. Picture of strip domains in grain of Fe (111) with texture. The strips are parallel to the average direction of the magnetization in the large domains [264].

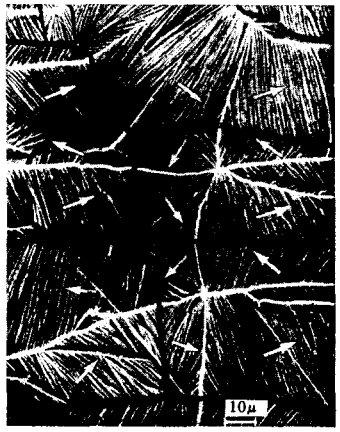

FIG. 20. Picture of domain structure of a film, demonstrating the appearance of Bloch lines on the inhomogeneities of a film [109].

were obtained by suitable control of the conditions. In the differently oriented crystals, the domain walls had different directions; in addition, even the density of the ties on the walls with cross ties were different. Analogous investigations[46] were performed on Fe films. Located in each Bloch wall were 1.5 crystallites (dimension 200—300 Å) in the case of 90° walls and three crystallites for 180° walls. In this case M_S rotates jumpwise over the width of the wall from crystallite to crystallite. Holes and defects of the films are also inhomogeneities that can bend and obstruct the walls. In Fig. 20, a number of Bloch lines coincide with holes in the film.

An investigation of the domain structure in Fe films with fine grain (50 Å) during the course of heating[286] has shown that such films exhibit a superparamagnetic behavior. After heating to 300° C, the magnetic contrast disappeared, a fact attributed to the destruction of the exchange interaction between the grains as a result of thermal oscillations (Fig. 21). An analogous transition was observed in Ga-Au films[387].

When Fe-Ga films were heated to 400° C, the ordinary domain structure disappeared and a speckled structure appeared[287,288]. The vanishing of the domain structure in a definite temperature interval is attributed to the presence of magnetic compensation of the antiferromagnetic interaction between the Fe and Ga atoms[289].

Investigations[290,129] of Ni films have revealed a very strong dependence of the domain structure on the crystallite dimensions.

The domain structure of Co films[229,171] depended strongly on the substrate temperature during the evaporation time. At a substrate temperature up to 100° C, the films had a speckled structure, and large domains appeared after demagnetization. Films evaporated at 250° C exhibited domain structure immediately.

The domain structure of Ni-Fe films was investigated in the temperature interval −110° − 540° C[110]. On cooling down to −110° C, the structure remained unchanged. During the time of heating, a motion of the walls (without an external field) was noted, probably as a result of the relief of the mechanical stresses in the film. After preliminary annealing at 400° C, the domain structure remained unchanged to 540° C. Heating caused a decrease of the width of the image of the walls, this being due mainly to the decrease of M_S with decreasing temperature. This yielded[47] the temperature dependence of M_S. The dimension of the domain structure of the Ni-Fe films also depends strongly on the crystallite dimensions. If the crystallite dimension is comparable with the width of the domain walls, then a very minute and irregular domain structure is obtained. The value of H_c in these films is large[58,189,375].

In thin (< 100 Å) Ni-Fe films, the domain structure is irregular, the walls are strongly curved, and zig-zag, spiral, and circular domains are observed[136,137]. In thick Ni-Fe films, a non-through domain structure was observed[296]. In 20% Ni-Fe films obtained by electric deposition on Cu, the domain structure varied greatly as a function of the lattice structure[130]. In films with face-centers lattices there is no EMA and the walls are irregular, and in films with body-centered lattices the domain structure consists of 90° and 180° boundaries. Electrically deposited films of permalloy with other compositions were investigated in[122].

The domain structure of films of the complex alloys 45% Co − 10% Mn − 45% Fe and 45% Co − 10% Cr − 45% Fe was investigated in[171,292]. A realignment of the domain structure of Fe—Ga and Co films following stretching and destruction of the domain walls was observed in[293,294]. The evolution of the domain structure in the course of sputtering of the films was observed in[386].

A regular structure of strip domains was also observed in evaporated films[61,265,295-310]. In a 95% Ni-Fe film 1200 Å thick, strip domains of width 1350 Å were observed[295]. For the alloy 81% Ni-Fe the critical thickness for the appearance of strip domains is 1700 Å[61]. An investigation of the occurrence of strip domains in films of 83% Ni-Fe of thickness 1500—3000 Å, obtained at different angles of incidence on the substrate, was carried out in[297-299]. At incidence angles 0—40°, the strip domains were perpendicular to the line of incidence of the substance and parallel to the domain walls. The image contrast of these domains is small (Fig. 22a). At incidence angles 50—60° there were very regular strip domains in the entire film, parallel to the line of incidence of the material

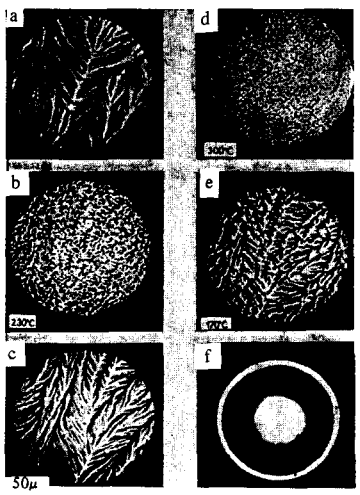

FIG. 21. Domain structure of Fe film with fine grain as a function of the temperature (a—e) and electron-diffraction pattern obtained at room temperature (f) [286].

and intersecting the domain walls. Their image contrast was very strong (Fig. 22b). These strip domains are due (i) to the appearance of 360° walls and their realignment and (ii) to the growth of the strip structure directly from the Bloch walls. The realignment of the strip domain structure was observed in[300].

In films of 40–100% Ni-Fe (d = 450–1800 Å) obtained by oblique evaporation (angle of incidence 57–75°), strip domains of width 1000–3500 Å were observed, in which the M_S component in the plane of the film was either parallel or perpendicular to the direction of incidence of the material[301]. In thin films there were no strip domains, but upon superposition of two thin films, such that their easy axes coincided, strip domains appeared in them. In Co-Al films, strip domains were observed at thicknesses 350–700 Å. Films with strip domains had a characteristic hysteresis loop, and a field of 500 Oe was needed for their saturation. These films had only a bcc structure[376].

A distinct domain structure is produced in multilayered films as a result of the interaction of the magnetic layers.[302] An investigation of multilayered films with an intermediate layer having a low Curie point (FeNi-PdCo-Co) has shown that the variation of the magnetization in PdCo with temperature (20–200° C) exerts an influence on the exchange interaction of the layers[303].

There is a short review devoted to the domain structures of films and foils[377].

VI. INVESTIGATION OF REVERSAL OF MAGNETIZATION OF FILMS

1. Magnetization reversing device. In the investigation of the processes of quasistatic magnetization reversal, the field should be homogeneous and it is necessary to be able to apply it at any angle to the easy axis. In the observation of reversal of magnetization in an electron microscope it is necessary, in addition, to exclude the influence of the magnetization-reversing field itself on the electron beam.

For a partial magnetization reversal of the film, the field of the objective was used in[56]. In[304,305], the field was produced by a coil whose axis was parallel to the optical axis, and the sample was inclined relative to the axis, as a result of which a field component appeared in the plane of the film and caused the displacement of the walls. Inclination of the film by 1–2° in the field of the objective also caused the appearance of a sufficient magnetic field in the plane of the film[258]. An inhomogeneous film up to 5 Oe was obtained in[257,250] by using a wire of 0.02 mm diameter passing near the film across the object holder. It was also proposed to use a set of wires located 1–2 mm below the sample, making it possible to obtain a rather uniform field up to 10 Oe[306]. This system was subsequently used[307] to apply pulsed fields. A homogeneous magnetic field parallel to the plane of the film is obtained from a pair of Helmholz coils[25,26,34,35,134,306,378], but since the electron beam is deflected by the field, observation during the time of adjustment of the field was difficult. To compensate for the shifts of the image by the action of the field on the beam, a device consisting of two pairs of oppositely-oriented coilc was used[184,185]. By choosing the ratio of the currents in each pair, a sufficient compensation of the image shift was obtained, but the image still remained distorted. The magnetization-reversal devices used in[308,309] contained two additional pairs of coils perpendicular to the first, and the entire system of coils could be rotated 360° around the film.

A complete illumination of the distortion and displacement of the image was attained[57,310] in a magnetizing device with three pairs of coils on E-shaped iron cores. The object was in the lower pair of coils. For each value of the defocusing it was possible to adjust the ratio of the coil currents and to obtain complete compensation. This device is extensively used[33,34,37,239-241,311,312] in conjunction with devices for heating, cooling, and stretching the sample. Motion picture photography of the reversal of film magnetization was carried out in[23,46,31,41,313-315].

2. Quasistatic reversal of magnetization. To explain the influence of different factors on the motion of the domain walls, investigations were made on films and foils prepared under different conditions. The growth of the domains as a result of the displacement of the walls begins with a certain definite value of the magnetization-reversing field H_0—the critical displacement field, the magnitude of which is inversely proportional to the film thickness[177]. The value of H_0 depends on the internal stresses in the film and on damage to the structure of the film[316]. In deformed films and in cold-rolled foils the walls move jumpwise, when the external field increases, whereas in annealed films the motion of the walls is smoother and occurs in weaker fields. It is assumed that the dislocations also hinder the motion of the walls. Strong interaction of the domain walls with the dislocations was observed in antiferromagnets[317,318], where the attachment of the walls was so strong that the domain structure hardly responded to fields up to 9000 Oe. An analogous "rigid" domain structure was observed in electrolytically deposited CoP films with coercive force ~1300 Oe[319]. The influence of dislocations in Co and Ni films was negligible[250].

The large influence of the grain boundaries on the domain structure in Fe foils was demonstrated in[267,268].

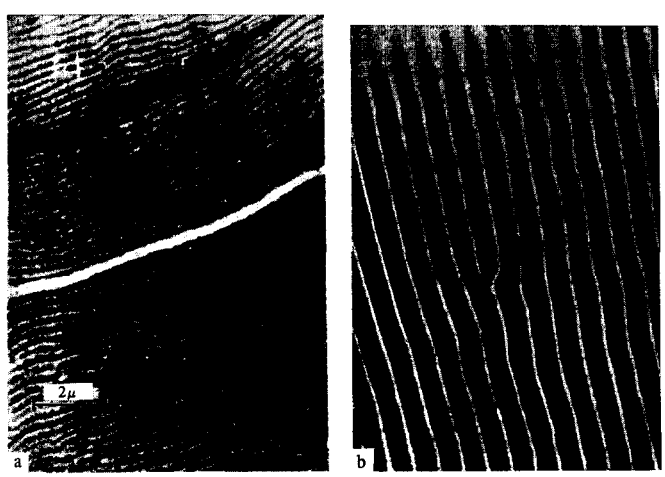

FIG. 22. a) Strip domain structure of permalloy film 2100 Å thick, evaporated at an angle of incidence of the atoms on the substrate of 20°; b) strip domain structure of permalloy film 3100 Å thick, evaporated at an incidence angle 60° [298].

The influence of inclusions and defects (holes) is even stronger[313]. The influence of inhomogeneities on the motion of domain walls can be regarded as the cause of the reproducibility of the positions of the walls in the film following partial reversal of magnetization[320]. Reversible wall motion was observed, however, also in a single-crystal Fe film of high purity[56], where the homogeneity of the structure was apparently much higher. The role of the inhomogeneities also accounts for the fact that the location the wall produced when the the magnetization is rotated in different directions is quite definite and is revealed by the rotation of the ripple even long before the wall is produced[321]. The crystal structure of the film exerts a strong influence on the formation and growth of the nuclei: in an Ni film with grain dimensions <500 Å, reversal of magnetization proceeded with a growth of a small number of nuclei and with wall motion over large distances, whereas in the case of large grain ($\sim$3000 Å) many nuclei with dimensions of several microns were produced[184]. The influence of a Cr sublayer in Co-Cr films on the coercive force was investigated in[322]. The grains of Co and H_c increase with increasing Cr thickness. The magnetic structure after the reversal of magnetization becomes more and more complicated. At large H_c, the magnetization reversal of the films was due more to the formation of new nuclei than to growth of those already formed.

When the sample is heated[47,110], and sometimes even under the influence of an electron beam[315], the motion of the walls is smoother and occurs in weaker fields. An interesting change in the process of magnetization reversal of Ni-Fe polycrystalline films and of Fe and Co polycrystalline and single-crystal films was observed when the sample was cooled with liquid helium to 4°K[323-327]. At 300°K, the reversal of magnetization occurred with formation of nuclei and with growth of these nuclei as a result of the displacement of the walls by Barkhausen jumps of $\geq 10\ \mu$, and no changes occurred in the domain structure in a constant magnetic field. In the temperature range 30—4°K, the magnetization reversal proceeds in an entirely different manner, the magnitude of the jump decreases to $\leq 0.1\ \mu$ and an aftereffect appears, in that the motion continues in a constant field. The details of the wall motion depend on the type of boundary. When the temperature is decreased from 300 to 4°K, increases take place in the wall-starting field, in the coercive field (by a factor 3—4), and in the field of nucleus formation (by 1.5—3 times). The rate of displacement in a constant field increases exponentially with increasing field, and the argument of the exponential decreases with decreasing temperature[328].

The motion of the domain wall is influenced also by stray fields of neighboring walls, provided the latter are sufficiently close. This is particularly strongly pronounced in two-layer magnetic films[305,329-330]. So long as the walls in both layers remain far from each other, their displacement is independent, however, as soon as the two walls become aligned, these two interacting walls continue to move together. If the coercive forces of both layers are different, then the motion of such interacting walls occurs in a field sufficient to displace the walls in a low-coercivity field, so that the coercive force of a two-layer film is equal to the smaller of the coercive forces of the layers[331]. A more detailed investigation[332,333] has shown that there is a magnetostatic interaction between the layers, so that a joint local rotation of the magnetization in the layers also occurs. In domains located in different layers, the magnetization is established in one direction, and the stray fields resulting from the formation of unlike magnetic charges on the roughnesses of the layers, are closed thereby. If the magnetization vectors in the middles of both walls are antiparallel, then the layer walls coincide exactly; if the orientation of the vectors coincides, then the walls are displaced by 0.5—1.5 μ. Different mutual positions of the walls are given in[334].

In some cases, the displacement of the wall is accompanied by a change in the wall structure. It was noted[23] that cross ties appear on a simple wall, presumably as a result of its motion over a section of the film with strong mechanical stresses. Under the influence of an increasing field directed perpendicular to the wall with cross ties, the transverse Bloch lines move along the wall, so that the Neel sections of the wall, with magnetization directed along the field, increase[314]. In a transverse alternating field the Bloch lines "shake,"[309] and this is accompanied by the phenomenon of "slipping" of the wall. The difference between the wall motion under the influence of the field along the easy and difficult axis lies in the fact that in the former case it is not accompanied by a change in the structure of the wall, and in the latter a realignment takes place[335]. When the film magnetization is reversed along the easy axis after the Neel walls turn into walls with cross ties, the number of ties increased and become maximal when the wall turns into a 180° one[336].

Unlike the magnetization reversal of ordinary films ($H_c < H_k$) along the easy axis, which is effected by growth of the nuclei and displacement of the walls (Fig. 23), rotation processes predominate in the case of magnetization reversal along directions close to the difficult axis[184,329,337-339]. In this case, when the saturating field decreases, rotation takes place in opposite directions and domain walls perpendicular to the field and to the difficult axis are produced. The reason for the oppositely-directed rotation is the dispersion of the anisotropy axes and the fluctuation of the magnetization vector. The stray field of the produced domain walls blocks the rotation process (Fig. 24). The magnetization

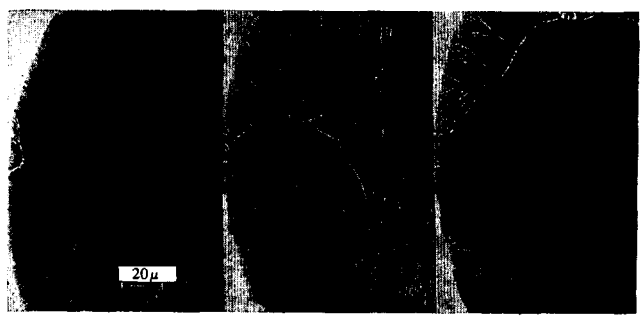

FIG. 23. Reversal of magnetization of Ni film 350 Å thick along the easy axis. The magnetization-reversing field increases from left to right [135].

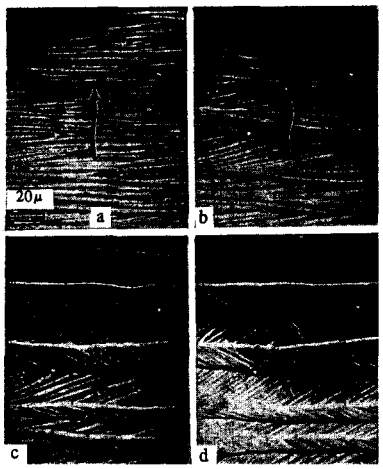

FIG. 24. Occurrence of a blocked structure in the reversal of the magnetization of a permalloy film saturated beforehand along the difficult axis. The field H increases along the difficult axis (field direction ↑): a) H = 7 Oe; b) H = 6 Oe; c) H = 5 Oe; d) H = 4 Oe [184].

reversal of inverse films ($H_c > H_k$) along the easy axis is analogous[321,340], except that in this case the "disintegration" of the magnetization and the formation of domain walls perpendicular to the field occurs upon application of an inverse field $\sim H_k$. The blocking produced thereby is lifted by the displacement of the domain boundaries and by motion of the Bloch lines. The reversal of the magnetization of inverse films along the difficult axis is similar to their magnetization reversal along the easy axis[177,341-343].

Partial rotation and blocking cause also formation of so-called labyrinth domains in the case of magnetization reversal at a large angle to the easy axis of a film saturated beforehand along the easy axis[340]. In the case of magnetization reversal of magneto-isotropic Ni-Fe films sputtered in a rotating field, the labyrinth structure is typical and the behavior of such films is similar to that of inverse films[245]. Various domain configurations produced by quasistatic magnetization reversal at different angles to the easy axis are shown in[135]. Thus, Fig. 25 shows the magnetization reversal of a section of a film with radial anisotropy, obtained by annealing with an electron beam. The magnetization of different sections of the film is reversed differently, depending on the mutual direction of the anisotropy axis and of the magnetization-reversing field.

The details of the mechanism of rotation of the fine structure were observed in[344]. Using the model of the small-angle walls, the results can be represented as an irreversible displacement and hysteresis of the waves of the fine structure of the magnetization.

The influence of the dispersion of the magnetization on the magnetization-reversal processes was investigated in[110,219,216]. It was found that the minimum of the coercive force of the films corresponds to a minimum of the wavelength of the fine structure of the magnetization. At an angular dispersion amplitude less than 13°, the magnetization reversal along the easy axis proceeds via displacement of the 180° walls, and along the difficult axis by rotation, which is almost reversible in weak fields. There were no 180° boundaries in the case of weakly pronounced anisotropy and large dispersion, and the structure took the form of intersecting light and dark lines. In a film whose magnetization is reversed along the difficult axis, the width of the domains decreased with increasing dispersion, and the residual magnetization increased[345].

The magnetization reversal of films having two equivalent easy-magnetization axes is somewhat more complicated. Such films include epitaxially-grown single-crystal films of Fe, Ni, Co, and Ni-Fe. The details of the magnetization-reversal process as a function of the orientation of the applied field relative to the crystallographic axes and of the film thickness have been discussed in sufficient detail in[169,224,311,346,252,347,248]. Biaxial anisotropy was obtained[348] also in polycrystalline Ni-Fe films.

Notice should be taken of the electron-microscopic observations of an interesting effect of the motion of domain walls—"the slipping of the walls"—namely the motion of walls in field weaker than critical under the influence of two fields, one constant along the easy magnetization axis and smaller than H_c, and the other alternating along the difficult-magnetization axis. In an electron microscope this was observed for the first time in[308]. Further investigations have demonstrated the creep of cross-tie walls in permalloy films. The details of the behavior of a cross-tie wall under the influence of fields along the easy and difficult magnetization axes were observed in[379]. Creep of Neel walls was also observed[350]. Whereas the application of bipolar pulses produced on the walls cross ties and Bloch lines, unipolar pulses did not change the wall structure, although creep did take place. The mechanism of this process is not clear. In films annealed with an electron beam, the wall creep process changed[121]. An investigation of films with larger anisotropy dispersion[351] has shown that the mechanism of the process differs from that observed earlier.

3. Investigation of fast reversal of magnetization. The ease with which the electron beam can be controlled and the fact that a very large temporal resolution is possible in principle in a transmission electron microscope (the time of interaction of the electron with the film of thickness 10^3 Å is approximately 10^{-15} sec) uncovers great possibilities for the investigation of dynamic processes, particularly for the study of fast reversal of magnetization of thin magnetic films.

Such investigations can be carried out with the aid of a stroboscopic electron microscope[320,352,353], the operating principle of which consists in the following. An electric beam illuminates the sample periodically with short pulses (strobe-pulses), in synchronism with

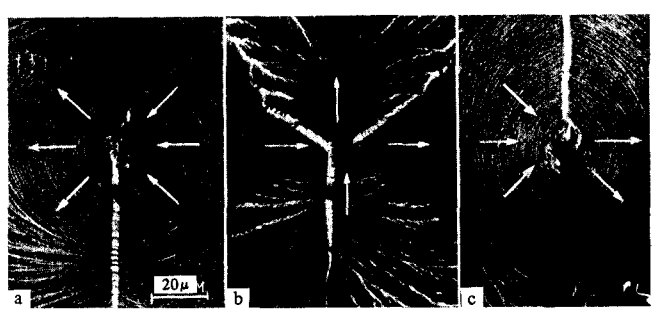

FIG. 25. Section of film with radial anisotropy before (a), during (b), and after (c) the reversal of magnetization [135].

the periodic magnetization-reversal field applied to the specimen. An image is produced on the screen only during the time of action of the strobe pulse. What is seen on the screen at a fixed phase shift of the strobe pulse relative to the magnetization-reversal field is a stationary image, averaged over the time of the strobe pulse and corresponding to the instant of observation (naturally, the reproducibility of the process must be sufficiently rigorous, or otherwise the picture becomes blurred). Under conditions of rigorous reproducibility of the process, the sharpness of the image will be determined by the extent to which the state of the sample changes during the time of the strobe pulse. By varying the shift between the strobe pulse and the magnetization-reversing field, it is possible to observe different instants of the development of the dynamic process.

The stroboscopic microscope mode can be realized by controlling the beam either in the space between the cathode and the modulator in the electron gun, or else on leaving the gun, using deflecting fields. In the former case the electron gun is shut off by a negative voltage between the cathode and the modulator, and is turned on by pulses fed through a pulse transformer[320,352-360] or through a decoupling capacitor[361,307,362,363]. The temporal resolution obtained so far (minimum duration of the strobe pulse) is 10 nsec using a transformer and ~2 nsec using a capacitor.

In the second case, the electron gun is on all the time and the electron beam is controlled by an electronic shutter[364]. The time resolution attained so far is ~10 nsec[356,358,365,366]. Advantages of controlling the beam in the gun is the independence of image quality on the wave form of the strobe pulse and the increase of the beam current by pulsed operation of the gun. On the other hand, if electronic shutters are used, important advantages are the simplicity the apparatus and the large operating range of strobe-pulse durations.

A very interesting fact was revealed by the investigation of the magnetization reversal in the stroboscopic mode, namely, the dynamic domain pictures and the local direction of the magnetization vector repeat from period to period of the magnetization-reversal signal with a high degree of accuracy. The reproducibility is obtained not only in the case of magnetization reversal in weak fields, but also in reversal from the state of saturation by fields amounting to $(2-3)H_k$[307,362,363], when the formation of the domain structure occurs anew each time. This can apparently be attributed to the fact that, owing to the different inhomogeneities of the film, the magnetization-reversal process proceeds in a certain definite manner, which is energywise more convenient, and the reversal process develops in this favored manner if the initial conditions and the magnetization-reversal field remain unchanged.

A number of recent investigations were devoted to the dynamics of magnetization reversal of thin magnetic films in a stroboscopic transmission electron microscope. The large sensitivity to the magnetic inhomogeneities of the thin magnetic films, the higher resolution, and the higher contrast make the stroboscopic electron microscope quite promising in comparison with stroboscopic magneto-optical installations.

A study was made[354] of the influence of the amplitude of a sinusoidal magnetization-reversing field applied at a small angle to the easy-magnetization axis, on the domain structure of the film. With increasing field amplitude, the domain decreased in width, and at still larger field amplitudes they turned into narrow island domains, whose configuration remained practically unchanged when the instant of observation was varied. Such a stabilization of the domain structure can be attributed to the blocking of the domain walls by the appearance of magnetic charges in them. With further increase of the field amplitude, the domain structure disintegrated.

The important role played by the magnetic charges produced on the domain walls upon reversal of magnetization is illustrated by Fig. 26. In this case two fields were applied to the film, a constant restoring field, which caused complete vanishing of the domain structure in the static mode, and a pulsed reversing field. When both fields are applied, it turns out that prior to the action of the pulsed fields (Fig. 26a) the film already has a domain structure. The magnetization-reversal process under the influence of the pulsed fields begins with a shift of the walls (walls M and N on Figs. 26a and 26b), and the contribution due to rotation is small. Subsequently (Figs. 26c and 26d) the process develops as a result of rotation of the magnetization, and by the end of the pulse many of the domain walls disappear, and the magnetization tends to turn into the direction of the action of the pulsed fields. The pulsed field gives rise to the production of island domains of inverse magnetization (A, B, C, and D in Figs. 26c and 26d). They are very stable and are apparently pinned on inhomogenei-

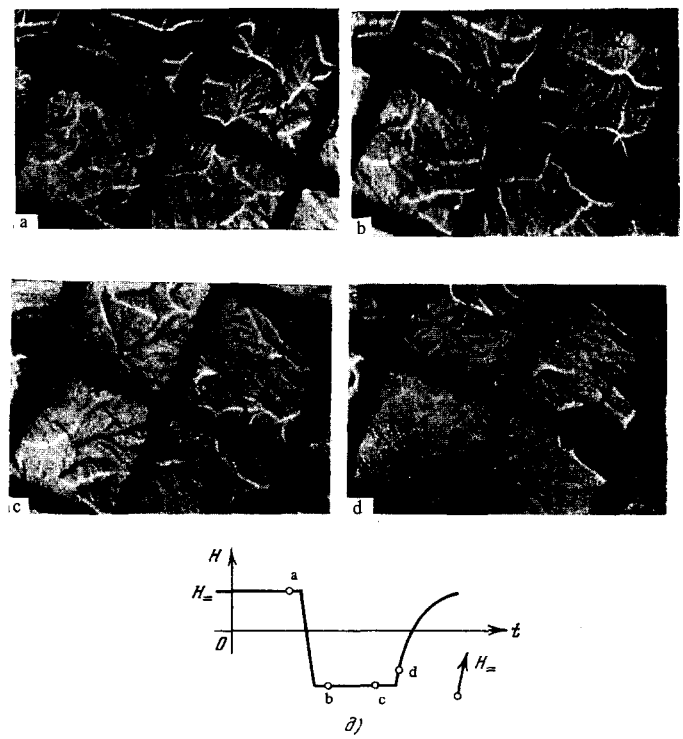

FIG. 26. a–d) Stroboscopic micrograms of the dynamic domain structure of a permalloy film 300 Å thick under the influence of a constant and a pulsed field at an angle to the easy-magnetization axis; e) time plot of the magnetic fields. Repetition frequency 4.1 kHz, strobe-pulse duration 0.5 μsec, t_{bc} = 20 μsec, t_{cd} = 10 μsec, grid mesh 50μ [365].

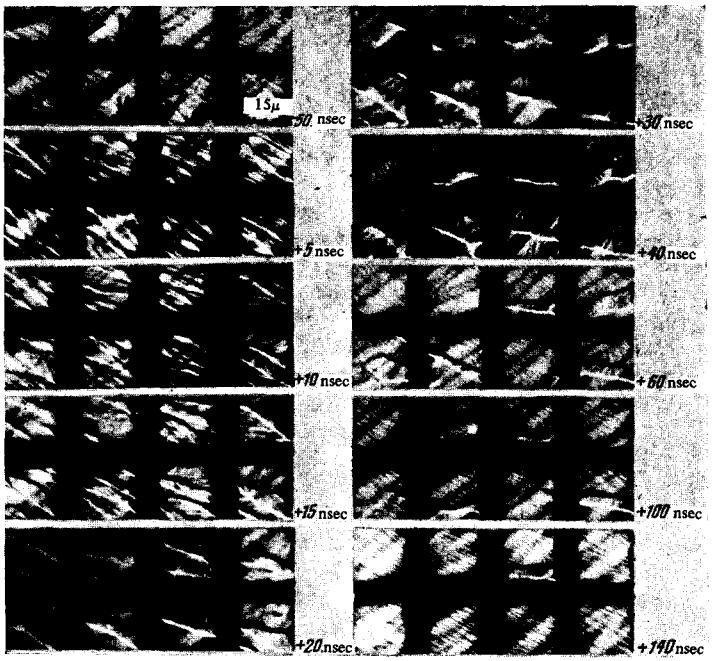

FIG. 27. Stroboscopic micrograms of magnetic structure of a permalloy film 250 Å thick, demonstrating the development of pulsed magnetization reversal of a film from the saturated state. Repetition frequency 50 kHz, strobe-pulse duration 2 nsec, grid mesh 33μ. The field H_S acts at a small angle to the easy magnetization axis. The numbers correspond to the instant of observation, in nanoseconds, relative to the start of the magnetization-reversal pulse [362].

ties. Their stray fields influence the rotation of the magnetization in the neighboring sections and prevent the magnetization from aligning itself with the field. In quasistatic magnetization reversal, island domains are usually not produced in these spots of the film, so that their production is determined not only by the presence of inhomogeneities but also by the very development of the dynamic process. The reconstruction of the structure is quite slow and is due mainly to the rotation of the magnetization, which causes the appearance of domain boundaries that subsequently maintain their positions practically constant. The slow development of the process is due primarily to the fact that magnetic charges appear on the wall as a result of different rotations of magnetization in the neighboring domains. These charges increase the "rigidity" of the wall and block the rotation of the magnetization in the neighboring domains. The walls begin to move only after the charges are removed.

By decreasing the duration of the strobe pulses to 2 nsec it was possible to observe the reversal of the films from the saturated state to the antisaturated state under the action of strong pulsed fields[307,362]. Figure 27 shows the stages of the film reversal process at a small angle to the easy magnetization axis. The process developed as a result of incoherent rotation that led to the formation of domains perpendicular to the field. The number of boundaries then decreased, and subsequently the final rotation of the magnetization occurred simultaneously with the longitudinal shortening of the domains. This interesting phenomenon of longitudinal vanishing of domains was observed for the first time.

Naturally, such information cannot be obtained either by motion picture photography in the ordinary mode, or with the aid of stroboscopic magneto-optical devices, although the latter do make it possible to observe the development of the process in the entire film[367]. In this sense the stroboscopic microscope, which gives a sharp local picture, and the stroboscopic magneto-optical setup, complement each other.

It should be noted that the magnetization reversal under the action of a series of single pulses of smaller amplitude differs radically from the process in Fig. 27. In this case the walls are produced along the easy magnetization axis, and each pulse causes a growth of the nuclei and a lateral motion of the walls, which is equivalent to the quasistatic behavior. Therefore results on intermittent magnetization reversal[368] must apparently be treated cautiously and not generalized to include the region of strong fields.

[1] S. V. Vonsovskiĭ and Ya. S. Shur, Ferromagnetizm (*Ferromagnetism*), Moscow-Leningrad, Gostekhizdat, 1948; in the translation collection: Magnitnaya struktura ferromagnetikov (Magnetic Structure of Ferromagnets), ed. by S. V. Vonsovskiĭ, Moscow, IL, 1959; in: "Magnitnaya struktura ferromagnetikov" (Magnetic Structure of Ferromagnets) ed. by L. V. Kirenskiĭ, Novosibirsk, SO AN SSSR, 1960; S. V. Vonsovskiĭ, Usp. Fiz. Nauk **90**, 491 (1966) [Sov. Phys.-Uspekhi **9**, 874 (1967)]; Magnetizm (Magnetism), Moscow, Nauka, 1971.

[2] W. Andrä, Z. Frait, V. Kamberský, Z. Málek, V. Rösler, W. Schüppel, P. Süda, L. Valenta and G. Vogler, Phys. stat. sol. **2**, 345 (1962).

[3] M. Pratton, Magnetic Thin Films (Russ. transl.), Sudostroenie, 1967.

[4] R. F. Soohoo, Magnetic Thin Films, Harper, 1964.

[5] R. Carey and E. D. Isaac, Magnetic Domains and Techniques for their Observation, Academic Press, New York—London, 1966.

[6] R. D. Heidenreich, Fundamentals of Transmission Electron Microscopy, Interscience, 1964; P. Hirsch et al., Electron Microscopy of Thin Crystals, Butterworth, 1966.

[7] H. Pfisterer and E. Fuchs, Siemens-Zs. 41, 572 (1967).
[8] V. A. Buravikhin and V. I. Popov, in: Fizika magnitnykh plenok (Physics of Magnetic Films), No. 1, ed. by L. V. Kirenskiĭ, Irkutsk, IPI, 1967, p. 91.
[9] P. J. Grundy and R. S. Tebble, Adv. Phys. 17, 153 (1968).
[10] V. I. Petrov, G. V. Spivak and O. P. Pavlyuchenko, Usp. Fiz. Nauk 102, 529 (1970) [Sov. Phys.-Uspekhi 13, 766 (1971)].
[11] Y. Aharonov and D. Bohm, Phys. Rev. 115, 485 (1959).
[12] W. Ehrenberg and R. E. Siday, Proc. Phys. Soc. B62, 8 (1949).
[13] R. G. Chambers, Phys. Rev. Lett. 5, 3 (1960).
[14] H. A. Fowler and L. Marton, et al., J. Appl. Phys. 32, 1153 (1961).
[15] H. Boersch, H. Hamisch, D. Wohlleben and K. Grohmann, Phys. Verh. 11, 179 (1960).
[16] H. Boersch, H. Hamisch, K. Grohmann and D. Wohlleben, Zs. Phys. 165, 79 (1961).
[17] W. Bayh, Zs. Phys. 169, 492 (1962).
[18] H. Boersch, H. Hamisch, D. Wohlleben and K. Grohmann, Zs. Phys. 159, 397 (1960).
[19] H. Boersch, H. Hamisch, D. Wohlleben and K. Grohmann, Zs. Phys. 164, 55 (1961).
[20] H. Boersch, H. Hamisch, K. Grohmann and D. Wohlleben, Zs. Phys. 167, 72 (1962).
[21] M. E. Hale, H. W. Fuller and H. Rubinstein, J. Appl. Phys. 0, 789 (1959).
[22] H. Boersch and H. Raith, Naturwiss. 46, 574 (1959).
[23] H. W. Fuller and M. E. Hale, J. Appl. Phys. 31, 308S (1960).
[24] H. W. Fuller and M. E. Hale, J. Appl. Phys. 31, 1699 (1960).
[25] D. H. Warrington, J. M. Rodgers and R. S. Tebble, Phil. Mag. 7, 1783 (1962).
[26] E. Fuchs, Zs. angew. Phys. 14, 203 (1962).
[27] V. G. Pyn'ko, Prib. Tekh. Eksp. No. 1, 178 (1964).
[28] O. P. Pavlyuchenko and V. I. Petrov, Izv. AN SSSR, ser. fiz. 30, 817 (1966).
[29] S. N. Kaverina and G. I. Levin, in: Nauch. tr. In-ta metallofiz. AN USSR 19, 132 (1964).
[30] V. N. Pushkar', O. A. Zaĭchuk and A. G. Lesnik, Izv. AN SSSR, ser. fiz. 29, 615 (1965).
[31] V. I. Popov, ibid. 29, 673 (1965).
[32] L. I. Chernyshova and G. I. Belik, Prib. Tekh. Eksp. No. 5, 170 (1969).
[33] JEOL News 2, 1 (1964).
[34] V. G. Pyn'ko, Prib. Tekh. Eksp. No. 6, 212 (1965).
[35] M. D. Coutts and H. Weinstein, J. Appl. Phys. 37, 5014 (1966).
[36] E. Fuchs, Naturwiss. 47, 392 (1960).
[37] V. A. Buravikhin and D. I. Voskoboĭnik, see[8], p. 114.
[38] M. Hibino and S. Maruse, Proc. 6th Intern. Congr. Electron Microscopy, Kyoto, vol. 1, 1966, p. 621.
[39] G. I. Belik and L. I. Chernyshova, in Tonkie magnitnye plenki v vychislitel'noĭ tekhnike i radiotekhnike (Magnetic Thin Films in Computation and Radio Engineering), vol. 2, Krasnoyarsk, IF SO AN SSSR, 1970, p. 159.
[40] H. W. Fuller and M. E. Hale, J. Appl. Phys. 31, 238 (1960).
[41] M. S. Cohen, J. Appl. Phys. 36, 1060, 1602 (1965).
[42] G. W. Wilson, Brit. J. Appl. Phys. 14, 160 (1963).
[43] R. H. Wade, Brit. J. Appl. Phys. 14, 398 (1963).
[44] V. I. Petrov, N. N. Sedov and G. V. Spivak, Izv. AN SSSR, ser. fiz. 32, 1185 (1968).
[45] M. J. Bowman and V. H. Meyer, J. Phys. E3, 329 (1970).
[46] L. Reimer, Zs. angew. Phys. 18, 373 (1965).
[47] T. Ichinokawa, Proc. 5th Intern. Congr. Electron Microscopy, Philadelphia, vol. 1, 1962, II-8.
[48] W. Liesk, Zs. angew. Phys. 14, 200 (1962).
[49] E. Fuchs, Naturwiss. 48, 450 (1961).
[50] V. Drahos and A. Delong, 3rd Czechosl. Conf. Electron. and Vacuum Phys. Trans., Prague, 1967, p. 655.
[51] Y. Sakaki and S. Maruse, Proc. 4th Intern. Congr. Electron Microscopy, London, vol. 1, 1958, p. 9.
[52] P. Pilod and F. Sonier, J. microscopie 7, 313 (1968).
[53] R. H. Wade and J. P. Guigay, Proc. 4th Europ. Conf. Electron Microscopy, Rome, vol. 1, 1968, p. 159.
[54] M. S. Cohen, J. Appl. Phys. 39, 1149 (1968).
[55] W. Pitsch, Proc. 3rd Europ. Conf. Electron Microscopy, Prague, pt. A, 1964, p. 291.
[56] J. T. Michalak and R. C. Glenn, J. Appl. Phys. 32, 1261 (1961).
[57] E. Fuchs and W. Liesk, Optik 19, 307 (1962).
[58] M. S. Cohen, J. Appl. Phys. 34, 1841 (1963).
[59] R. I. Tagirov and A. A. Glazer, Tr. Vsesoyuznogo simpoziuma po apparature i metodam issledovaniya tonkikh magnitnykh plenok (Proc. All-union Symp. on Apparatus and Methods of Investigating Thin Magnetic Films), Krasnoyarsk, IF SO AN SSSR, 1968, p. 188.
[60] P. Vigier and P. C. Haymann, Compt. rend. B264, 1565 (1967).
[61] D. S. Lo, A. L. Olson, C. D. Olson, H. N. Oredson, W. J. Simon and E. J. Torok, J. Appl. Phys. 38, 1344 (1967).
[62] S. Tsukahara, JEOL News 9e(2), 8 (1970).
[63] H. Boersch, H. Raith and D. Wohlleben, Zs. Phys. 159, 388 (1960).
[64] W. J. S. Blackburn, G. H. Curtis and R. P. Ferrier, J. Phys. E2, 570 (1960).
[65] G. Dupouy and F. Perrier et al., Compt. rend. B266, 1064 (1968).
[66] G. Dupouy, see[53], p. 3.
[67] A. Seguela, Proc. 7th Intern. Congr. Electron Microscopy, Grenoble, vol. 2, 1970, p. 609.
[68] M. S. Cohen, J. Appl. Phys. 38, 4966 (1967).
[69] R. H. Wade, J. de phys. 29, Suppl. 2–3, C2-95 (1968).
[70] D. Gabor, Proc. Phys. Soc. 64, 449 (1951).
[71] A. Olivei, Optik 30, 27 (1969).
[72] M. J. Bowman and V. H. Meyer, J. Phys. E3, 927 (1970).
[73] H. Mahl and W. Weitsch, Zs. Naturforsch. 15a, 1051 (1961); G. A. Bassett and A. Keller, Phil. Mag. 9, 817 (1964); R. H. Wade and J. Silcox, Appl. Phys. Lett. 8, 7 (1966); Phys. stat. sol. 19, 57 (1967).
[74] R. P. Ferrier, Adv. Optical and Electron Microscopy 3, 155 (1969).
[75] R. H. Wade, Phys. stat. sol. 19, 847 (1967).
[76] R. P. Ferrier, see[55], p. 115.
[77] R. P. Ferrier and R. H. Wade, Proc. Intern. Conf. Magnetism, Nottingham, 1964, p. 873.

[78] R. H. Wade, Bull. Soc. fr. minéral. cristallogr. 90, 479 (1967).
[79] M. J. Goringe and J. P. Jakubovics, Phil. Mag. 15, 393 (1967).
[80] J. P. Jakubovics, Phil. Mag. 10, 277 (1964).
[81] J. P. Jakubovics, Ph. D. Thesis (University of Cambridge, 1965).
[82] M. Wilkens, Phys. stat. sol. 9, 255 (1965).
[83] J. P. Jakubovics, Phil. Mag. 13, 85 (1966).
[84] H. Boersch, see[47], II-1.
[85] D. Wohlleben, Phys. Lett. 22, 564 (1966).
[86] D. Wohlleben, J. Appl. Phys. 38, 1292 (1967).
[87] D. Wohlleben, J. Appl. Phys. 38, 3341 (1967).
[88] J. P. Guigay and A. Bourret, Compt. rend. B264, 1389 (1967).
[89] H. Wahl, Optik 28, 417 (1969).
[90] J. P. Guigay and R. H. Wade, Phys. stat. sol. 29, 799 (1968).
[91] O. Bostanjoglo and W. Vieweger, Phys. stat. sol. 32, 311 (1969).
[92] H. Boersch, J. Geiger and H. Raith, Zs. Phys. 160, 66 (1960).
[93] D. Wohlleben, J. Appl. Phys. 39, 1197 (1968).
[94] D. Wohlleben, J. Appl. Phys. 41, 1344 (1970).
[95] H. Dietze and H. Thomas, Zs. Phys. 163, 523 (1961).
[96] S. Middelhoek, J. Appl. Phys. 34, 1054 (1963).
[97] E. Feldtkeller and E. Fuchs, Zs. angew. Phys. 18, 1 (1964).
[98] H. Weik and P. Hemenger, Zs. angew. Phys. 19, 314 (1965).
[99] R. Collete, J. Appl. Phys. 35, 3294 (1964).
[100] W. F. Brown, Jr. and A. E. La Bonte, J. Appl. Phys. 36, 1380 (1965).
[101] C. D. Olson, H. N. Oredson and E. J. Torok, J. Appl. Phys. 38, 1349 (1967).
[102] A. Aharoni, J. Appl. Phys. 38, 3196 (1967).
[103] H. N. Oredson and E. J. Torok, IEEE Trans. Magnet. MAG-4 (1), 32 (1968).
[104] R. Kirchner and W. Döring, J. Appl. Phys. 39, 855 (1968).
[105] Th. Ricker and K. H. Locherer, Zs. angew. Phys. 26, 223 (1969).
[106] A. E. La Bonte, J. Appl. Phys. 40, 2450 (1969).
[107] A. Hubert, Phys. stat. sol. 32, 519 (1969); 38, 699 (1970).
[108] E. E. Huber, D. O. Smith and J. B. Goodenough, J. Appl. Phys. 29, 294 (1958).
[109] W. Bürger, Phys. stat. sol. a4, 723 (1971).
[110] V. A. Buravikhin and V. I. Popov, Izv. AN SSSR, ser. fiz. 29, 682 (1965).
[111] H. Sato, S. Shinozaki and R. S. Toth, see[77], p. 798.
[112] V. A. Buravikhin and V. I. Popov, Phys. stat. sol. 16, 657 (1966).
[113] V. A. Buravikhin and P. I. Krukover, see[8], p. 145.
[114] Ya. M. Pogosyan et al., Izv. AN Arm.SSR (Fizika) 5, 103 (1970).
[115] V. I. Popov, V. A. Buravikhin et al., Fiz. Met. Metallov. 29, 548 (1970).
[116] Ya. M. Pogosyan, A. G. Shishkov and R. V. Telesnin, ibid. 30, 880 (1970).
[117] V. I. Popov, V. A. Buravikhin, V. P. Karabanova and V. I. Shvetsov, Materialy Mezhdunar. simpoziuma po fizike tonkikh magnitnykh plenok (Proc. Internat. Symp. on Physics of Magn. Thin Films), Irkutsk, IPI, 1968, p. 396.
[118] V. A. Buravikhin, V. P. Karabanova et al., in: Fizika magnitnykh plenok (Physics of Magnetic Films), No. 4, Irkutsk, IPI, 1971, p. 110.
[119] E. J. Torok, A. L. Olson and H. N. Oredson, J. Appl. Phys. 36, 1394 (1965).
[120] S. Middelhoek, J. Appl. Phys. 33, 1111 (1962).
[121] E. J. Torok, H. N. Oredson and W. J. Simon, J. Appl. Phys. 41, 1338 (1970).
[122] E. Fuchs and A. Politycki, Zs. angew. Phys. 13, 541 (1961).
[123] M. D. Coutts and H. L. Pinch, J. Appl. Phys. 34, 2113 (1963).
[124] M. Mohiuddin, Brit. J. Appl. Phys. 17, 789 (1966).
[125] V. P. Karabanova, in: Fizika magnitnykh plenok (Physics of Magnetic Films), No. 3, Irkutsk, IPI, 1970, p. 8.
[126] E. A. Gorokhov, V. P. Karabanova and V. I. Popov, Fiz. Met. Metallov. 30, 1288 (1970).
[127] V. A. Bouravikhin, E. A. Gorokhov, V. P. Karabanova and V. I. Popov, a) Thesis Intern. Conf. Magnetism, Grenoble, 1970, MaF11; b) see[125], p. 3.
[128] H. Sato, R. W. Astrue and S. S. Shinozaki, J. Appl. Phys. 35, 822 (1964).
[129] W. J. S. Blackburn and R. P. Ferrier, J. Appl. Phys. 37, 1163 (1966).
[130] G. A. Jones, D. P. Oxley and R. S. Tebble, Phil. Mag. 11, 993 (1965).
[131] N. I. Sivkov and V. G. Pyn'ko, Izv. AN SSSR, ser. fiz. 34, 1586 (1970).
[132] S. Tsukahara, H. Kawakatsu and T. Taoka, Jernkontor. Ann. 155 (8) 468 (1971).
[133] G. A. Jones and B. K. Middleton, J. Phys. D2, 685 (1969).
[134] R. H. Wade, Phil. Mag. 10, 49 (1964).
[135] H. Pfisterer, Phys. Blätter 20, 312 (1964).
[136] E. Feldtkeller and W. Liesk, Zs. angew. Phys. 14, 195 (1966).
[137] M. S. Cohen, J. Appl. Phys. 34, 1221 (1963).
[138] P. Vigier and P. Haymann, Phys. stat. sol. 34, 649 (1969).
[139] D. C. Hothersall, Phys. stat. sol. 34, 677 (1969).
[140] P. Vigier and P. Haymann, see[67], p. 615.
[141] L. D. Landau and E. M. Lifshitz, Phys. Zs. Sowjetunion 8, 153 (1935).
[142] H. Weik and P. M. Hemenger, Phys. Lett. 13, 210 (1964).
[143] P. M. Hemenger and H. Weik, J. Appl. Phys. 36, 1052 (1965).
[144] R. H. Wade, J. Appl. Phys. 37, 366 (1966).
[145] L. Reimer and H. Kappert, Zs. angew. Phys. 26, 58 (1969).
[146] T. Suzuki, C. H. Wilts and C. E. Patton, J. Appl. Phys. 39, 1983 (1968).
[147] T. Suzuki and C. H. Wilts, J. Appl. Phys. 40, 1216 (1969).
[148] J. P. Guigay, cm. [67], p. 605.
[149] D. Wohlleben, Report at the 3rd Intern. Coll. Magnetic Magnetic Films, Boston (1967) (private communication).
[150] D. H. Warrington, Phil. Mag. 9, 261 (1964).
[151] G. V. Spivak, L. A. Bogdanova and V. I. Petrov, Tezisy 7-i Vsesoyuznoĭ konferentsii po élektronnoĭ mikroskopii (Abstracts of the 7th All-union Conference on Electron Microscopy), Section II. Solid State,

Moscow, 1969, p. 86.
[152] V. I. Petrov, G. V. Spivak and A. Sh. Aĭrapetov, Izv. AN SSSR, ser. fiz. 34, 1582 (1970).
[153] L. Reimer and H. Kappert, Zs. angew. Phys. 27, 165 (1969).
[154] L. Reimer and K. H. Sommer, Zs. Naturforsch. 23a, 1569 (1969).
[155] T. Suzuki and M. Wilkens, see[67], p. 611.
[156] T. Suzuki and M. Wilkens, Phys. stat. sol. a3, 43 (1970).
[157] T. Suzuki, Abstracts 4th Intern. Coll. Thin Magnetic Films, Prague, 1970, 9.2.
[158] V. R. Matricardi, W. G. Lehmann, N. Kitamura and J. Silcox, J. Appl. Phys. 38, 1297 (1967).
[159] A. S. Keh and Ch. A. Johnson, J. Appl. Phys. 34, 2670 (1963).
[160] D. C. Hothersall, see[67], p. 617.
[161] K. Schaffernicht, Zs. angew. Phys. 15, 275 (1963).
[162] Th. Ricker, a) Phys. stat. sol. 30, K93 (1968); b) Thesis Intermag-69, Amsterdam, 1969, 1.1.
[163] T. Suzuki and A. Hubert, Phys. stat. sol. 38, K5 (1970).
[164] D. C. Hothersall, Phil. Mag. 20, 89 (1969).
[165] S. P. Ray and D. I. Paul, J. Appl. Phys. 41, 5238 (1970).
[166] S. Mader and A. S. Nowick, Thin Solid Films 1, 45 (1968).
[167] T. Suzuku, cm.[127a], LuF2; J. de phys. 32, Suppl. 2–3, C1-134 (1971).
[168] R. H. Wade, Proc. Phys. Soc. 79, 1237 (1962).
[169] L. V. Kirenski and V. G. Pynko, et al., Phys. Stat. Sol. 17, 249 (1966).
[170] L. V. Kirenskiĭ, V. G. Pyn'ko et al., Izv. AN SSSR, ser. fiz. 31, 716 (1967).
[171] G. I. Belik and L. I. Chernyshova, Izv. Vuzov (Fizika) 9, 62 (1968).
[172] G. I. Belik et al., Izv. AN SSSR, ser. fiz. 34, 1592 (1970).
[173] M. K. Savchenko, D. A. Lapteĭ et al., Izv. Vuzov (Fizika) 7, 70 (1969).
[174] H. Boersch, H. Raith and H. Weber, Zs. Phys. 161, 1 (1961).
[175] H. Kappert, Zs. angew. Phys. 29, 139 (1970).
[176] F. Lenz and E. Krimmel, Zs. Phys. 163, 356 (1961).
[177] E. Feldtkeller, Zs. angew. Phys. 15, 206 (1963).
[178] V. I. Petrov, N. N. Sedov and G. V. Spivak, see[117], p. 160.
[179] K. J. Harte and M. S. Cohen, J. Appl. Phys. 40, 1218 (1969).
[180] M. S. Cohen and K. J. Harte, J. Appl. Phys. 40, 3597 (1969).
[181] J. M. Rodgers, see[77], p. 866.
[182] R. S. Tebble, see[77], p. 859.
[183] P. J. Grundy, Brit. J. Appl. Phys. 16, 409 (1965).
[184] E. Fuchs, Zs. angew. Phys. 13, 157 (1961).
[185] L. Reimer, Zs. angew. Phys. 13, 143 (1961).
[186] G. A. Jones, Brit. J. Appl. Phys. 15, 875 (1964).
[187] M. J. Marcinkowski and R. M. Poliak, Acta Metallurg. 12, 179 (1964).
[188] P. V. Vigier and P. Haymann, Compt. rend. B267, 22 (1968); B273, 745 (1971).
[189] E. Feldtkeller, Zs. angew. Phys. 17, 121 (1964).
[190] K. D. Leaver, Thin Solid Films 2, 149 (1968).
[191] H. Rother, Zs. Phys. 168, 148 (1962).
[192] P. Shnupp, Ann. Phys. 14, 1 (1964).
[193] K. J. Harte, Thesis (Harvard University, Cambridge, Mass., 1964).
[194] H. Hoffmann, J. Appl. Phys. 35, 1790 (1964).
[195] K. J. Harte, J. Appl. Phys. 37, 1295 (1966).
[196] K. J. Harte, J. Appl. Phys. 39, 1503 (1968).
[197] H. Hoffmann, Phys. stat. sol. 4, K93 (1964).
[198] E. Feldtkeller, see[77], p. 837.
[199] S. Tsukahara, J. Phys. Soc. Japan 23, 189 (1967).
[200] T. Suzuki and C. H. Wils, J. Appl. Phys. 39, 1151 (1968).
[201] T. Suzuki, Phys. stat. sol. 37, 101 (1970).
[202] F. G. West and C. L. Simmons, J. Appl. Phys. 37, 1283 (1966).
[203] J. J. Chang, A. R. von Neida and C. J. Calbick, J. Appl. Phys. 37, 1472 (1966).
[204] A. Baltz and W. D. Doyle, J. Appl. Phys. 35, 1814 (1964).
[205] E. Feldtkeller, see[77], p. 846.
[206] T. Suzuki, J. Phys. Soc. Japan 28, 920 (1970).
[207] S. Maruse and M. Hibino, Zs. angew. Phys. 27, 183 (1969).
[208] T. Suzuki, Report at the Meeting on Lorentz Microscopy, Grenoble, 1970 (private communication).
[209] R. Ajelan, H. Kappert and L. Reimer, Zs. angew. Phys. 30, 80 (1970).
[210] L. Reimer and H. Kappert, Report at the Meeting on Lorentz Microscopy, Grenoble, 1970 (private communication).
[211] H. G. Badde, H. Kappert and L. Reimer, Zs. angew. Phys. 30, 83 (1970).
[212] L. I. Chernyshova, I. S. Édel'man and N. I. Sivkov, Izv. AN SSSR, ser. fiz. 34, 1589 (1970).
[213] I. S. Édel'man and L. I. Chernyshova, Fiz. Met. Metallov. 28, 440 (1969); see[157], 6.6.
[214] Ya. M. Pogosyan, L. A. Bezirganyan et al., ibid. 30, 733 (1970).
[215] H. L. Gaigher, Zs. Phys. 223, 257 (1969).
[216] A. Baltz, see[77], p. 845.
[217] T. Fujii, S. Uchiyama, E. Yamada and Y. Sakaki, Japan. J. Appl. Phys. 6, 1 (1967).
[218] L. I. Chernyshova, G. I. Belik and A. G. Baranov, see[39], p. 163.
[219] L. V. Kirenskiĭ and R. V. Sukhanova et al., Izv AN SSSR, ser. fiz. 30, 1035 (1966).
[220] L. V. Kirenskiĭ et al., ibid. 30, 1038 (1966).
[221] R. V. Sukhanova, S. V. Kan and A. S. Komalov, Fiz. Met. Metallov. 27, 558 (1969).
[222] R. J. Spain and I. B. Puchalska, J. Appl. Phys. 35, 824 (1964).
[223] S. Tsukahara and H. Kawakatsu, J. Phys. Soc. Japan 21, 313 (1966).
[224] G. A. Jones, Phys. stat. sol. 19, 811 (1967).
[225] L. V. Kirenskiĭ, R. V. Sukhanova et al., Izv. AN SSSR, ser. fiz. 30, 50 (1966).
[226] P. Escudier and F. Biragnet et al., Phys. stat. sol. 16, 295 (1966).
[227] D. S. Lo, J. Appl. Phys. 37, 1289 (1966).
[228] D. S. Lo, J. Appl. Phys. 37, 3246 (1966).
[229] L. V. Kirenskiĭ, V. G. Pyn'ko et al., Izv. AN SSSR, ser. fiz. 30, 34 (1966).
[230] Y. Yokoyama, T. Sato and T. Magashima, J. Phys. Soc. Japan 21, 1839 (1966).
[231] I. B. Puchalska, A. Sukiennicki and K. Branska,

Phys. stat. sol. **14**, K119 (1966).
[232] I. B. Puchalska, see[77], p. 870.
[233] I. B. Puchalska, A. Sukiennicki and T. Tymosz, Phys. stat. sol. **9**, 575 (1965).
[234] V. A. Buravikhin and V. I. Popov, Izv. AN SSSR, ser. fiz. **29**, 677 (1965).
[235] I. B. Puchalska and A. Sukiennicki, Phys. stat. sol. **21**, K57 (1967).
[236] R. V. Sukhanova, V. G. Pyn'ko and N. I. Sivkov, Izv. AN SSSR, ser. fiz. **31**, 435 (1967).
[237] V. A. Buravikhin, D. I. Voskoboĭnik et al., see[117], p. 341.
[238] S. Tsukahara and H. Kawakatsu, J. Phys. Soc. Japan **21**, 2551 (1966).
[239] P. Tischer, see[53], p. 353.
[240] H. Pfisterer, E. Fuchs and P. Tischer, Zs. angew. Phys. **27**, 179 (1969).
[241] V. A. Buravikhin and V. I. Popov, Fiz. Met. Metallov. **20**, 146 (1965).
[242] T. Iwata, R. J. Prosen and B. E. Gran, J. Appl. Phys. **38**, 1364 (1967).
[243] G. Bate and D. E. Speliotis et al., see[77], p. 816.
[244] D. E. Speliotis and G. Bate et al., J. Appl. Phys. **36**, 972 (1965).
[245] E. Fuchs and W. Zinn, J. Appl. Phys. **34**, 2557 (1963).
[246] D. C. Hothersall, Phil. Mag. **20**, 433 (1969).
[247] L. V. Kirenskiĭ, V. G. Pyn'ko and I. P. Antipin, Izv. AN SSSR, ser. fiz. **30**, 46 (1966).
[248] N. I. Sivkov and V. G. Pyn'ko, see[39], p. 146.
[249] D. C. Finbow and D. A. Havard, Phys. stat. sol. **38**, 541 (1970).
[250] J. Silcox, Phil. Mag. **8**, 7 (1963).
[251] P. J. Grundy, Phil. Mag. **12**, 335 (1965).
[252] L. V. Kirenskiĭ, V. G. Pyn'ko and N. I. Sivkov, Izv. AN SSSR, ser. fiz. **30**, 91 (1966).
[253] P. J. Grundy and R. S. Tebble, Proc. Phys. Soc. **81**, 971 (1963).
[254] P. J. Grundy and B. Johnson, J. Phys. **D2**, 1279 (1969).
[255] P. J. Grundy, R. S. Tebble and D. C. Hothersall, a) J. Phys. **D4**, 174 (1971); b) Digests Intermag. Conf. Denver, U.S.A., 1971, 10.12.
[256] J. Silcox, Phil. Mag. **8**, 1395 (1963).
[257] J. Silcox, see[47], II-5.
[258] J. M. Rodgers, Thesis (University of Sheffield, 1964).
[259] P. J. Grundy, Thesis (University of Sheffield, 1964).
[260] J. P. Jakubovics, Phil. Mag. **14**, 881 (1966).
[261] R. Gemperle and A. Gemperle, Phys. stat. sol. **26**, 207 (1968).
[262] P. J. Grundy, Phil. Mag. **14**, 901 (1966).
[263] P. J. Grundy and R. S. Tebble, J. Appl. Phys. **35**, 923 (1964).
[264] A. Bourret and D. Dautreppe, Phys. stat. sol. **13**, 559 (1966).
[265] R. W. De Blois, J. Appl. Phys. **36**, 1647 (1965).
[266] A. Bourret and M. Kleman, Colloq. internat. Centre nat. rech. scient., No. 167, 1968, p. 167.
[267] J. Kallor, D. I. Paul and A. Tobin, J. Appl. Phys. **37**, 4979 (1966).
[268] A. G. Tobin and D. I. Paul, J. Appl. Phys. **40**, 3611 (1969).
[269] M. J. Marcinkowski and R. M. Poliak, Phil. Mag. **8**, 1023 (1963).
[270] A. F. Smith, J. Phys. **D7**, 1044 (1970).
[271] J. P. Jakubovics, see[77], p. 875.
[272] J. P. Jakubovics, Phil. Mag. **10**, 675 (1964).
[273] M. J. Marcinkowski and R. C. Glenn, Brit. J. Appl. Phys. **15**, 523 (1964).
[274] A. J. Lapworth, J. P. Jakubovics and G. S. Baker, see[127a], MaE5; J. de phys. **32**, Suppl. 2–3, C1-259 (1971).
[275] L. V. Kirenskiĭ, L. M. Obraztsova et al., see[151], p. 90.
[276] L. Kirensky, L. Obrazstsova and V. Pynko, see[157], 5.3; Czechosl. J. Phys. **B21**, 513 (1971).
[277] O. Bostanjoglo and W. Vieweger, Phys. stat. sol. **39**, 471 (1970).
[278] J. Dash and W. R. Bitler, J. Appl. Phys. **37**, 1095 (1966).
[279] V. I. Izotov and L. M. Utevskiĭ, Fiz. Met. Metallov. **25**, 751 (1968).
[280] G. Remaut and P. Delavignette et al., J. Appl. Phys. **35**, 1351 (1964).
[281] G. Remaut, A. Lagasse and S. Amelinckx, Phys. stat. sol. **7**, 497 (1964).
[282] Van Landuyt and S. Amelinckx, Appl. Phys. Lett. **4**, 15 (1964).
[283] M. S. Cohen, IEEE Trans. Magnet. **MAG-1**, 156 (1965).
[284] J. P. Auradon, J. microscopie **5**, 1 (1966).
[285] M. Hibino and S. Maruse, Japan J. Appl. Phys. **8**, 366 (1969).
[286] G. A. Jones, Brit. J. Appl. Phys. **17**, 383 (1966).
[287] V. A. Buravikhin, D. I. Voskoboĭnik et al., see[8], p. 142.
[288] V. A. Buravikhin, D. I. Boskoboĭnik et al., in: Fizika magnitnykh plenok (Physics of Magnetic Films), No. 2, Irkutsk, IPI, 1970, p. 13.
[289] D. I. Voskoboĭnik, A. A. Nedel'ko and V. N. Shelkovnikov, see[8], p. 137.
[290] L. Reimer, J. Ficker, T. Pieper and E. Wossner, Zs. angew. Phys. **15**, 204 (1963).
[291] L. V. Kirenskiĭ, R. V. Sukhanova and V. G. Pyn'ko, Fiz. Met. Metallov. **21**, 308 (1966).
[292] L. I. Chernyshova, G. I. Belik et al., Izv. Vuzov (Fizika) **8**, 145 (1969).
[293] V. A. Buravikhin, D. I. Voskoboĭnik et al., see[117], p. 335.
[294] V. G. Kazakov, P. I. Krukover et al., see[117], p. 418.
[295] T. Koikeda, K. Suzuki and S. Chikazumi, Appl. Phys. Lett. **4**, 160 (1964).
[296] R. J. Spain, Appl. Phys. Lett. **3**, 208 (1963).
[297] I. B. Puchalska and R. P. Ferrier, Thin Solid Films **1**, 437 (1968).
[298] R. P. Ferrier and I. B. Puchalska, Phys. stat. sol. **28**, 335 (1968).
[299] I. B. Puchalska, Acta Phys. Polon. **36**, 589 (1969).
[300] J. H. Bennett and R. P. Ferrier, see[67], p. 607.
[301] S. Tsukahara, J. Phys. Soc. Japan **28**, 62 (1970).
[302] E. Feldtkeller, J. Appl. Phys. **39**, 1181 (1968).
[303] L. Piche, J. Devenyi and O. Massenet, see[157], 5.2; Czechosl. J. Phys. **B21**, 510 (1971).
[304] I. B. Puchalska and R. J. Spain, see[47], II-6.
[305] I. B. Puchalska and R. J. Spain, Compt. Rend. **254**, 2937 (1962).
[306] R. H. Wade, Thesis (University of Cambridge, 1963).

[307] U. A. Durasova, O. S. Kolotov, I. S. Kolotov, V. I. Petrov, G. V. Spivak and R. V. Telesnin, see[162], 1.2; Izv. AN SSSR, ser. fiz. 34, 1580 (1970).
[308] M. S. Cohen, see[47], E-9.
[309] A. Green and R. M. Livesay, J. Sci. Instr. 42, 31 (1965).
[310] E. Fuchs and W. Liesk, West German Patent, cl. 21q, 37/10, No. 1144856.
[311] L. V. Kirenskiĭ, V. G. Pyn'ko et al., Fiz. Met. Metallov. 22, 380 (1966).
[312] Ya. M. Pogosyan et al., Zavod. lab. 36, 362 (1970).
[313] Ch. A. Johnson and R. C. Glenn, J. Appl. Phys. 37, 946 (1966).
[314] E. Fuchs and H. Pfisterer, see[47], II-4.
[315] L. Reimer, Zs. angew. Phys. 14, 193 (1962).
[316] T. S. Lin, IEEE Trans. Magnet. MAG-2, 438 (1966).
[317] P. Delavignette, R. Gevers and S. Amelinckx, see[55], p. 259.
[318] H. Zijlstra and H. B. Haanstra, J. Appl. Phys. 37, 1105, 2853 (1966).
[319] J. S. Salo and J. M. Carr, J. Electrochem. Soc. 109, 1040 (1962).
[320] G. V. Spivak, O. P. Pavlyuchenko and V. I. Petrov, Izv. AN SSSR, ser. fiz. 30, 793 (1966).
[321] E. Feldtkeller, Naturwiss. 48, 474 (1961).
[322] J. Daval and D. Randet, Digests Intermag. Conf. Washington, 1970, 5/4; IEEE Trans. Magnet MAG-6, 768 (1970).
[323] O. Bostanjoglo and H. Fichtner, Phys. stat. sol. 34, 511 (1969).
[324] O. Bostanjoglo, Phys. stat. sol. 37, 247 (1970).
[325] O. Bostanjoglo, P. Kreisel and A. Oelmann, Phys. stat. sol. 38, 607 (1970).
[326] O. Bostanjoglo, Phys. stat. sol. 38, 617 (1970).
[327] O. Bostanjoglo, P. Kreisel and A. Oelmann, see[67], p. 613.
[328] O. Bostanjoglo and P. Kreisel, Phys. stat. sol. a3, 393 (1970).
[329] I. B. Puchalska and R. J. Spain, Compt. rend. 254, 72 (1962).
[330] R. J. Spain and I. B. Puchalska, see[47], II-3.
[331] H. W. Fuller and L. R. Lakin, J. Appl. Phys. 34, 1069 (1963).
[332] E. Feldtkeller, E. Fuchs and W. Liesk, see[55], p. 295.
[333] E. Feldtkeller, E. Fuchs and W. Liesk, Zs. angew. Phys. 18, 370 (1965).
[334] F. Biragnet and J. Devenye et al., Phys. stat. sol. 16, 569 (1966).
[335] V. A. Buravikhin and V. I. Popov, Izv. Vuzov (Fizika) 4, 116 (1965).
[336] J. A. Jones, Brit. J. Appl. Phys. 16, 969 (1965).
[337] R. H. Wade, see[47], II-7.
[338] E. Feldtkeller, Zs. angew. Phys. 13, 161 (1961).
[339] T. A. Pogosyan, Ya. M. Pogosyan and P. A. Bezirganyan, Izv. AN Arm. SSR (Fizika) 5, 169 (1970).
[340] E. Feldtkeller, Elektron. Rechenanl. 3, 167 (1961).
[341] Ya. M. Pogosyan, T. A. Pogosyan and V. A. Mamyan, Izv. Arm. SSR (Fizika) 3, 378 (1968).
[342] T. A. Pogosyan, Ya. M. Pogosyan, ibid. 4, 8 (1969).
[343] T. A. Pogosyan, Ya. M. Pogosyan, and V. A. Mamyan, ibid. 4, 19 (1969).
[344] E. Feldtkeller, J. Appl. Phys. 34, 2646 (1963).
[345] V. M. Pushkar, Ukr. fiz. zh. 11, 806 (1966).
[346] N. I. Sivkov, V. S. Prokopenko and V. G. Pyn'ko, Izv. AN SSSR, ser. fiz. 30, 832 (1966).
[347] L. V. Kirenskiĭ and V. G. Pyn'ko, ibid. 30, 93 (1966).
[348] Y. Gondo, B. E. Gran and R. J. Prosen, J. Appl. Phys. 36, 1062 (1965).
[349] E. J. Torok, D. S. Lo, H. N. Oredson and W. J. Simon, J. Appl. Phys. 40, 1222 (1969).
[350] D. S. Lo and M. M. Hanson, IEEE Trans. Magnet. MAG-5, 115 (1969).
[351] Ya. M. Pogosyan, Z. M. Gzryan and S. A. Artyunyan, Fiz. Met. Metallov., 31, 417 (1971); in: Tonkie magnitnye plenki v vychislitel'noĭ tekhnike i radiotekhnike (Thin Magnetic Films in Computation and Radio Engineering), vol. 2, Krasnoyarsk, IF SO AN SSSR, 1971, p. 37.
[352] G. V. Spivac, O. P. Pavljutschenko and V. I. Petrov, Intern. Coll. Grundprobleme Physik dünner Schichten, Clausthal-Göttingen, 1965, S. 38.
[353] V. I. Petrov, G. V. Spivak and O. P. Pavluchenko, see[38], p. 615.
[354] V. I. Petrov, G. V. Spivak and O. P. Pavluchenko, Izv. AN SSSR, ser. fiz. 31, 362 (1967).
[355] G. V. Spivak, O. P. Pavlyuchenko and V. I. Petrov, Authors Certificate (Patent) No. 201541 (2.XI 1965).
[356] V. I. Petrov, G. V. Spivak, O. P. Pavluchenko and V. V. Shakmanov, see[53], p. 357.
[357] G. V. Spivak, E. M. Dubinina et al., Izv. AN SSSR, ser. fiz. 32, 1098 (1968).
[358] G. V. Spivak, O. P. Pavlyuchenko, V. I. Petrov et al., Tezisy Vsesoyuznogo simpoziuma po élektronnomikroskopicheskomy priborostreoniyu, Nauchnyĭ sovet po élektronnoĭ mikroskopii (Abstracts of All-union Symposium on Electron-Microscopy Instrument Building), Science Council on Electron Microscopy, SFTN AN SSSR, Sumy, 1968, p. 26.
[359] O. P. Pavlyuchenko and N. M. Salanskiĭ, see[151], p. 93.
[360] O. P. Pavlyuchenko and N. M. Salanskiĭ, Tezisy 7-i Vsesoyuznoĭ konferentsii po élektronnoĭ mikroskopii (Abstracts of 7th All-Union Conference on Electron Microscopy), Sec. I. Elektron Optics and Instrument Building, Science Council on Electron Microscopy, SFTN AN SSSR, Moscow, 1969, p. 3.
[361] Yu. A. Durasova, O. S. Kolotov et al., see[59], p. 399.
[362] U. A. Durasova, I. S. Kolotov, O. S. Kolotov, V. I. Petrov, G. V. Spivak and R. V. Telesnin, see[67], p. 619, and[157], 2.1; Czechosl. J. Phys. B21, 451 (1971).
[363] I. S. Kolotov, O. S. Kolotov, V. A. Pogozhev and R. V. Telesnin, see[127a]; LuF5.
[364] G. V. Spivak, V. V. Shakmanov, V. I. Petrov, A. E. Luk'yanov and S. I. Yakunin, Izv. AN SSSR, ser. fiz. 32, 1111 (1968).
[365] V. I. Petrov and G. V. Spivak, Zs. angew. Phys. 27, 188 (1969).
[366] V. I. Petrov, G. V. Spivak and V. Sh. Melamed, see[151], p. 92.
[367] M. H. Cryder and F. B. Humphrey, see[117], p. 316.
[368] P. D. Kim and L. A. Safonov, et al., see[151], p. 91.
[369] N. Minnaja, M. Nobile and F. Pedrielli, see[255a], 8.8.
[370] T. Suzuki and A. Seeger, Comm. Solid State Phys. 3, 128 (1970/1971).
[371] A. Aharoni, J. de phys. 32, Suppl. 2—3, C1-966 (1971).

[372] H. Kappert and P. Schmiesing, Phys. stat. sol. a4, 737 (1971).
[373] T. Suzuki and A. Seeger, Comm. Solid State Phys. 3, 173 (1971).
[374] T. Suzuki, Zs. Angew. Phys. 32, 75 (1971'.
[375] M. S. Cohen, J. Appl. Phys. 33, 2968 (1962).
[376] D. I. Norman, D. S. Lo and T. R. Johansen, J. Appl. Phys. 42, 1810 (1971).
[377] E. Feldtkeller, J. de phys. 32, Suppl. 2–3, C1-452 (1971).
[378] W. Bürger, Exper. Tech. Phys. 18, 217 (1970).
[379] W. Bürger, Phys. stat. sol. a4, 713 (1971).
[380] V. S. Prokopenko and G. G. Vasil'ev, Tezisy 8-i Vsesoyuznoĭ konferentsii po élektronnoĭ mikroskopii (Abstracts of the 8th All-Union Conference on Electron Microscopes), Vol. 1, Moscow, Znanie, 1971, p. 61.
[381] B. V. Vasil'ev and N. I. Sivkov, see[380], p. 61.
[382] D. I. Belik, D. A. Lapteĭ and M. K. Savchenko, see[380], p. 63.
[383] L. I. Chernyshova, M. S. Édel'man and N. I. Sivkov, see[380], p. 62.
[384] L. M. Obraztsova and V. G. Pyn'ko, see[380], p. 70.
[385] G. A. Jones, J. Phys. E4, 833 (1971).
[386] O. Bostanjoglo and A. Oelmann, Zs. angew. Phys. 32, 118 (1971).
[387] O. Bostanjoglo and K. Röhkel, Phys. stat. sol. a7, 387 (1971).

Translated by J. G. Adashko